iScience

CellPress
OPEN ACCESS

Article

Neuronal-enriched small extracellular vesicles trigger a PD-L1-mediated broad suppression of T cells in Parkinson's disease

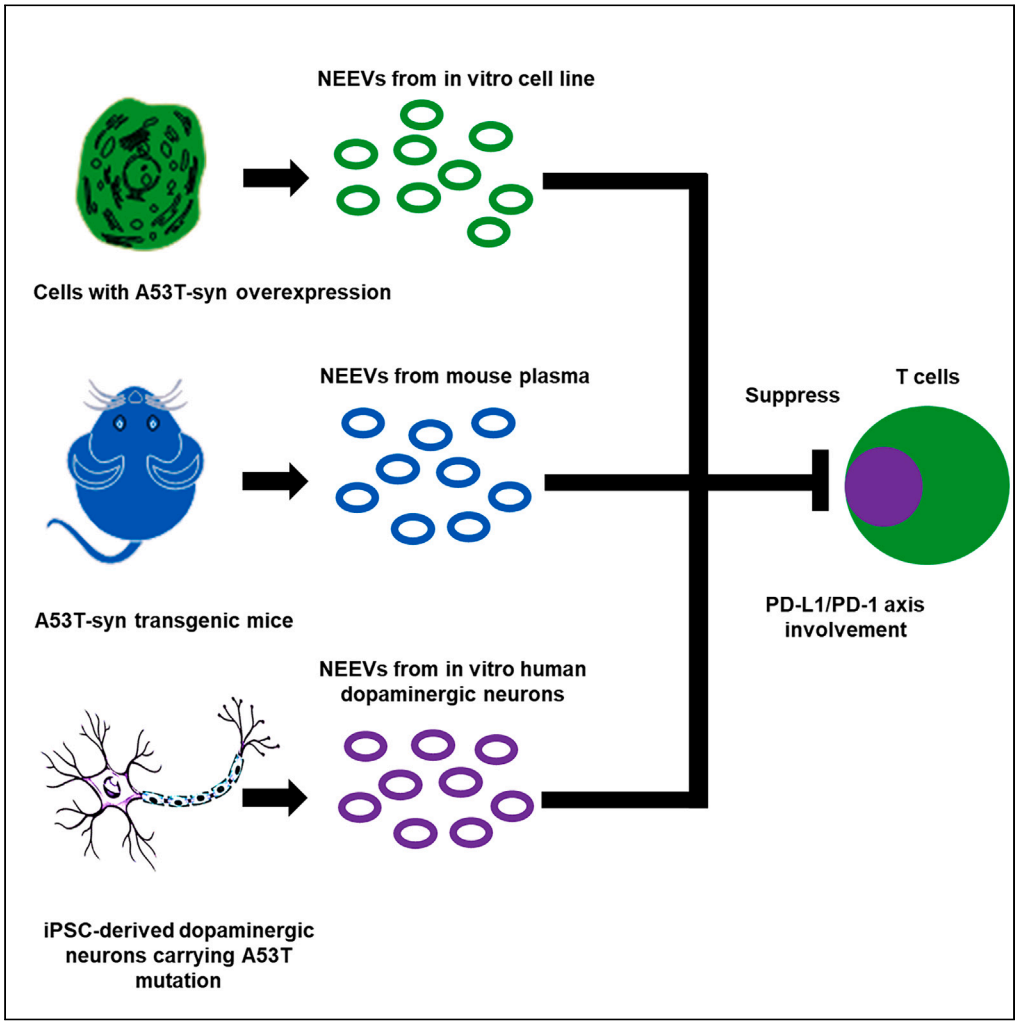

Zhichun Chen, Wenming Li, Bo Meng, ..., Zhexing Wen, Jun Liu, Zixu Mao

lj11128@rjh.com.cn (J.L.)
zmao@emory.edu (Z.M.)

Highlights

NEEVs derived from *in vitro* and *in vivo* PD models suppress $CD4^+$ and $CD8^+$ T cells

NEEVs isolated from PD models suppress Th1 and Th2 differentiation

The suppressed phenotype is associated with increased PD-L1 level in T cells

Blocking PD-L1 with an anti-PD-L1 antibody or BMS-1166 reverses T cell suppression

Chen et al., iScience 27, 110243
July 19, 2024
https://doi.org/10.1016/j.isci.2024.110243

iScience

CellPress
OPEN ACCESS

Article

Neuronal-enriched small extracellular vesicles trigger a PD-L1-mediated broad suppression of T cells in Parkinson's disease

Zhichun Chen,[1,2,3] Wenming Li,[1] Bo Meng,[1] Chongchong Xu,[4] Yiqi Huang,[5] Guanglu Li,[2] Zhexing Wen,[4,6] Jun Liu,[2,*] and Zixu Mao[1,6,7,8,*]

SUMMARY

Many clinical studies indicate a significant decrease of peripheral T cells in Parkinson's disease (PD). There is currently no mechanistic explanation for this important observation. Here, we found that small extracellular vesicles (sEVs) derived from *in vitro* and *in vivo* PD models suppressed IL-4 and INF-γ production from both purified $CD4^+$ and $CD8^+$ T cells and inhibited their activation and proliferation. Furthermore, neuronal-enriched sEVs (NEEVs) isolated from plasma of A53T-syn mice and culture media of human dopaminergic neurons carrying A53T-syn mutation also suppressed Th1 and Th2 differentiation of naive $CD4^+$ T cells. Mechanistically, the suppressed phenotype induced by NEEVs was associated with altered programmed death ligand 1 (PD-L1) level in T cells. Blocking PD-L1 with an anti-PD-L1 antibody or a small molecule inhibitor BMS-1166 reversed T cell suppression. Our study provides the basis for exploring peripheral T cells in PD pathogenesis and as biomarkers or therapeutic targets for the disease.

INTRODUCTION

Adaptive immunity plays an important role in Parkinson's disease (PD), and peripheral T lymphocytes are key players in the pathogenesis of the disease.[1,2] Recent evidence in two large-scale longitudinal cohorts has shown that lower peripheral lymphocyte count is associated with increased risk of PD.[3,4] Several studies indicate that the percentages of peripheral $CD3^+$ and $CD4^+$ T cell are reduced in clinical PD patients.[5–9] In addition, PD patients exhibit a reduced activation of peripheral $CD3^+$, $CD4^+$, and $CD8^+$ T cells[10,11] and reduced numbers of naive and regulatory $CD4^+$ and $CD8^+$ T cells.[12,13] Consistent with these, the levels of IL-4, IL-6, IL-10, tumor necrosis factor, and IFN-γ are reported to be reduced in the plasma of PD patients.[11] Recent new evidence further indicates that the levels of transcription factors important for $CD4^+$ T cell differentiation, including *T-bet*, *STAT3*, and *STAT4*, are also reduced in PD patients.[14] Therefore, the peripheral T cells in PD patients exhibit a suppressed phenotype in general although T cells infiltrating into the brain are reported to be cytotoxically activated.[15–18] However, the mechanism that underlies the broad suppression of peripheral T cells in PD remains elusive.

Exosome is a subtype of small extracellular vesicles (sEVs) with 30–200 nm diameter in size originated from multivesicular bodies, which are specialized endosomes containing membrane-bound intraluminal vesicles.[19,20] sEVs isolated by sequential centrifugation processes not only include exosomes (30–200 nm) but also contain a subpopulation of microvesicles between 50 and 300 nm in size. sEVs have been shown to deliver DNA, RNA, and proteins from the donor cells to acceptor cells, interstitial fluid, as well as blood circulation.[19,20] In cancers, sEV proteins and RNAs are known to mediate anti-tumor T cell immunity and promote tumor metastasis.[21–23] sEVs have also been shown to play an important role in multiple pathological processes and are associated with the clinical phenotypes of patients with neurodegenerative diseases, including Alzheimer's disease (AD), PD, dementia with Lewy bodies, and frontotemporal dementia/amyotrophic lateral sclerosis.[24–29] sEVs can induce the seeding and transmission of neurotoxic proteins including α-synuclein.[26,28,30,31] Moreover, the level of α-synuclein is significantly increased in plasma neuronal-enriched sEVs (NEEVs) of PD patients.[9,32–35] Reducing exosome biogenesis significantly suppresses the pathological propagation of α-synuclein in PD as well as Aβ in AD.[26,30,36] T cells from PD patients have been shown to respond to α-synuclein-derived peptides.[37] But it is not clear if and how sEVs modulate peripheral T cells in PD. In this study, we identified the role of NEEVs derived from models of PD in mediating a broad suppression of peripheral T cells and revealed the mechanism underlying this inhibitory process.

[1]Departments of Pharmacology & Chemical Biology and Neurology, Emory University School of Medicine, Atlanta, GA 30322, USA
[2]Department of Neurology and Institute of Neurology, Ruijin Hospital Affiliated to Shanghai Jiao Tong University School of Medicine, Shanghai 200025, China
[3]Department of Neurology, The Second Affiliated Hospital of Hainan Medical University, Haikou 570311, China
[4]Departments of Psychiatry and Behavioral Sciences and Cell Biology, Emory University School of Medicine, Atlanta, GA 30322, USA
[5]The Graduate Program in Neuroscience, Laney Graduate School, Emory University, Atlanta, GA 30322, USA
[6]Department of Neurology, Emory University School of Medicine, Atlanta, GA 30322, USA
[7]Center for Neurodegenerative Diseases, Emory University School of Medicine, Atlanta, GA 30322, USA
[8]Lead contact
*Correspondence: lj11128@rjh.com.cn (J.L.), zmao@emory.edu (Z.M.)
https://doi.org/10.1016/j.isci.2024.110243

RESULTS

sEVs derived from cells expressing A53T α-synuclein suppress T cells

To clarify the role of sEVs in regulating T cell function in PD, we over-expressed α-synuclein A53T mutant (A53T-syn) in mouse midbrain dopaminergic (DAergic) progenitor SN4741, human neuroglioma H4, and microglial HMC3 cell lines, and prepared sEVs from their culture media using sequential centrifugation processes.[38] The purified sEVs/exosomes were shown to have typical cup-shaped morphology and size by transmission electron microscopy (TEM) as previously reported[38] (Figure S1A) and expressed exosome markers, such as Alix, CD63, and TSG101 (Figures S1B–S1D and Datas S1–S3). A53T-syn expression led to higher level of A53T-syn in the total cell lysates and purified sEVs/exosomes (Figures S1B–S1D and Data S1–S3). We characterized the size distribution and concentrations of sEVs secreted by cultured cells using nanoparticle tracking analysis (NTA). As shown in Figures S1E–S1N, the control sEVs and A53T-syn sEVs purified from both SN4741 cells and HMC3 cells had a size distribution consistent with that of exosomes reported by previous studies.[39,40] The median diameters of A53T-syn sEVs were much larger than control sEVs while the concentrations of A53T-syn sEVs were lower than control sEVs (Figures S1E–S1N). These results suggested that A53T-syn modulated the biogenesis of sEVs by increasing their size and reducing their concentration.

To investigate the effects of A53T-syn sEVs on $CD4^+$ and $CD8^+$ T cells, we purified $CD4^+$ and $CD8^+$ T cells from mouse spleens using a negative selection method[41] and incubated them with A53T-syn sEVs isolated from media of SN4741 cells and assessed cytokine production by flow cytometry. To demonstrate that sEVs isolated from SN4741 cells can be internalized by cultured mouse T cells, we used a previously reported approach to label the sEVs with Dil dye[42] and tested whether Dil-labeled sEVs could be internalized by cultured mouse $CD4^+$ T cells. The Figure S2 showed the successful uptake of Dil-labeled control and A53T-syn sEVs by mouse $CD4^+$ T cells after incubation for 24 h (Figure S2). Then we found that A53T-syn sEVs derived from media of SN4741 cells significantly reduced the percentage of both $CD4^+$ and $CD8^+$ T cells positive for IL-4 and INF-γ compared with control sEVs (Figures S3A and S3B). A53T-syn sEVs derived from media of either H4 or HMC3 cells exhibited similar inhibitory effects on the cytokine production of $CD4^+$ and $CD8^+$ T cells (Figures S3C and S3D). These findings indicate that A53T-syn sEVs negatively regulates the cytokine production of both $CD4^+$ and $CD8^+$ T cells. Given the similar effects of A53T-syn sEVs isolated from different cell culture media, we chose SN4741 cells as the primary sEV source for the subsequent investigation.

NEEVs from A53T α-synuclein transgenic mice suppress T cells

Since α-synuclein A53T mutant dysregulates neuronal biogenesis of exosomes/sEVs, we tested the effects of NEEVs on T cells. We followed an experimental protocol as shown in Figure 1A. We initially isolated NEEVs from the plasma of wild-type mice (WT-NEEVs) and A53T α-synuclein transgenic mice (A53T-NEEVs) using L1 cell adhesion molecule (L1CAM, simply L1) antibody-coated superparamagnetic microbeads following the protocol as previously described.[33] Analysis of exosome/sEVs markers revealed that similar to sEVs isolated from cultured cells, plasma WT-NEEVs and A53T-NEEVs expressed exosome markers CD63 and TSG101, but the levels of Alix were low (Figures 1B and Data S4). We incubated the spleen cells, purified $CD4^+$ T cells, and purified $CD8^+$ T cells with plasma WT-NEEVs and A53T-NEEVs. The analysis showed that compared to WT-NEEVs, A53T-NEEVs significantly reduced the percentage of $CD45^+CD3^+$ T cells when incubated with murine spleen cells (Figure 1C). Moreover, this reduction was caused primarily by a significant decrease of $CD8^+$ T cell but not $CD4^+$ T cells (Figure 1C). Interestingly, consistent with the results shown in Figure S3, A53T-NEEVs significantly reduced the percentages of $CD4^+$ and $CD8^+$ T cells expressing either IL-4 or INF-γ when incubated with purified $CD4^+$ or $CD8^+$ T cells (Figures 1D and 1E). Based on these results, we further evaluated whether A53T-NEEVs reduced the activation or proliferation of $CD4^+$ and $CD8^+$ T cells. We found that the percentages of activated $CD4^+$ ($CD4^+CD44^+$) and $CD8^+$ ($CD8^+CD44^+$) T cells were significantly reduced by A53T-NEEVs compared to WT-NEEVs (Figures 1F and 1G). Furthermore, we also observed a decline in the percentages of CD4+Ki67+ and CD8+Ki67 + T cells with the treatment of A53T-NEEVs compared to WT-NEEVs (Figures 1H and 1I). We analyzed the geometric mean fluorescence intensity (MFI) for the above examined indices of all the flow cytometric presentations in Figures 1D–1I and found that A53T-NEEVs suppressed T cells compared to WT-NEEVs (Figure S4). These findings demonstrate that plasma A53T-NEEVs induce a T cell phenotype that is consistent with a broad suppression of both $CD4^+$ and $CD8^+$ cells.

sEVs isolated from media of human iPSC-derived DAergic neurons carrying A53T mutation suppress T cells

To strengthen the findings above, we tested the effects of sEVs isolated from culture media of human iPSC-derived DAergic neurons on T cells. For this study, we prepared sEVs from media of DAergic neurons derived from human iPSC carrying A53T mutation (A53T-DA neurons) or DA neurons of the same iPSC line with the A53T mutation corrected by CRISPR-Cas9 (WT-DA neurons). We first showed that DA neurons derived from human iPSCs expressed robust levels of DA neuronal markers tyrosine hydroxylase (TH) and pituitary homeobox 3 (PITX3) as assessed by immunofluorescence (Figure 2A) and *NURR1* and *VMAT2 mRNAs* by RT-qPCR (Figure 2B), indicating that most cells were matured DAergic neurons. Surprisingly, the level of soluble α-synuclein was lower in A53T-DA neurons compared to WT-DA neurons (Figures 2C and Data S5). We isolated sEVs from the culture media of WT-DA and A53T-DA neurons (WT-DA sEV and A53T-DA sEV, respectively) and confirmed that they expressed comparable high levels of CD63 and TSG101, but the levels of Alix were relatively low (Figures 2D and Data S6). We then compared the effects of WT-DA sEVs and A53T-DA sEVs on T cells and found that compared to WT-DA sEVs, exposure of purified murine $CD4^+$ or $CD8^+$ T cells to A53T-DA sEVs significantly reduced the percentages of T cells with CD4+IL-4+, CD4+INF-γ+, CD8+IL-4+, or $CD8^+$ INF-γ+ (Figures 2E and 2F). The suppression of cytokines by A53T-DA sEVs was also accompanied by the reduction of T cell activation and proliferation since the percentages of T cells with $CD4^+CD44^+$, $CD8^+CD44^+$, CD4+Ki67+, or $CD8^+$ Ki67+ were all significantly reduced by A53T-DA sEVs (Figures 2G–2J). Thus, A53T-syn sEVs from human iPSC-derived DA neurons also causes a general suppression of T cells.

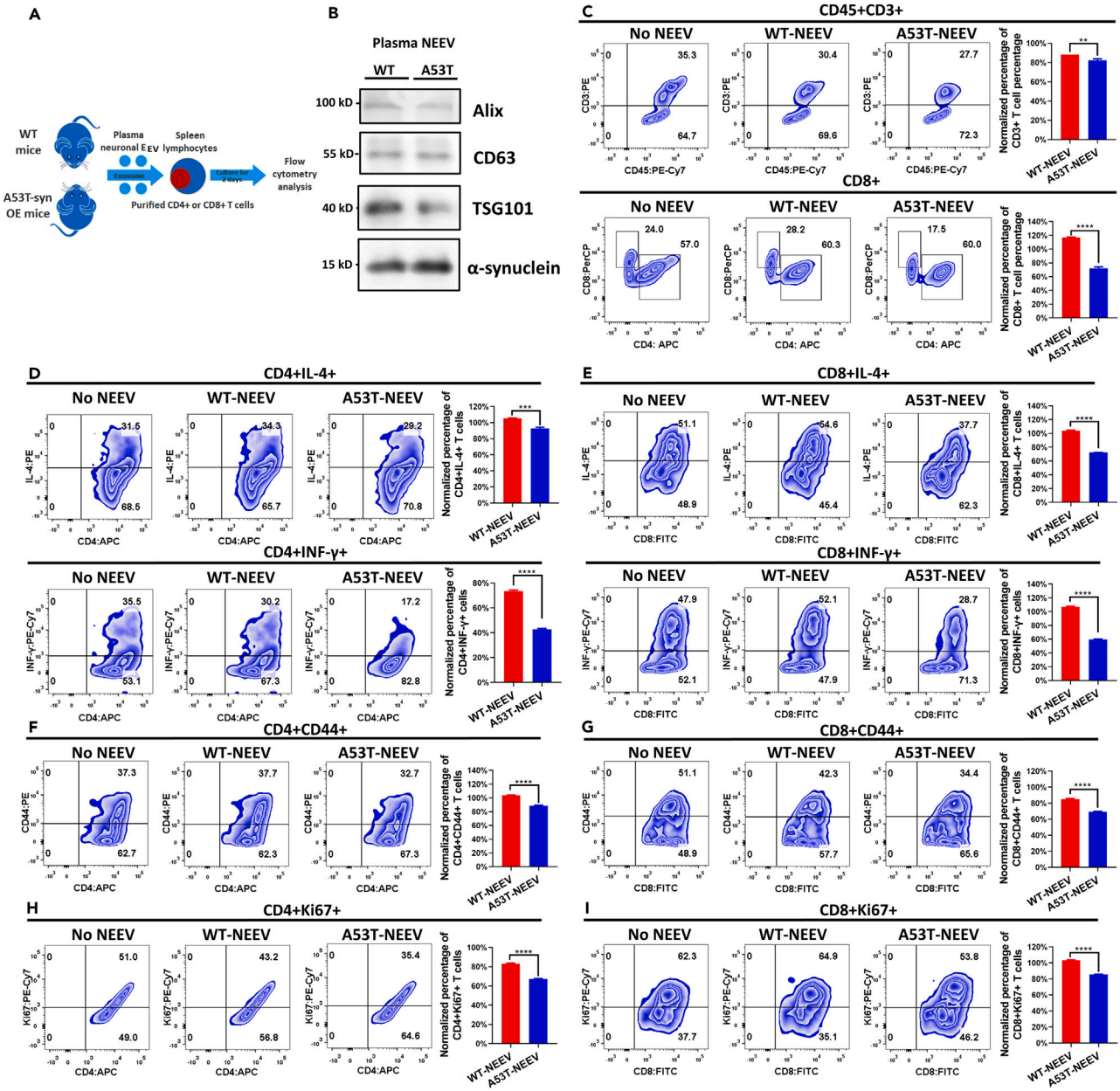

Figure 1. NEEVs isolated from the plasma of A53T-syn transgenic mice suppress T cells

(A) Experimental protocol for the treatment of isolated spleen lymphocytes or $CD4^+$ and $CD8^+$ T cells with NEEVs from the plasma of A53T-syn transgenic mice (A53T-syn overexpression [OE] mice).

(B) The expressions of exosome markers in NEEVs isolated from the plasma of WT and A53T-syn transgenic mice. The raw data for all blots were shown in Data S4.

(C) A53T-NEEVs reduce the percentages of $CD3^+$ and $CD8^+$ T cells in the total spleen lymphocytes. Total mouse spleen lymphocytes were treated with NEEVs (10 μg/mL; WT-NEEV and A53T-NEEV were purified from the plasma of WT mice or A53T α-synuclein transgenic mice, respectively) for 48 h before flow cytometry analysis for the percentages of cells expressing CD3 or CD8.

(D–I) A53T-NEEVs reduce the percentages of CD4+INF-γ+, CD4+IL-4+, CD8+INF-γ+, and CD8+IL-4+ T cells (D andE), the percentages of $CD4^+CD44^+$ and $CD8^+CD44^+$ T cells (F andG), and the percentages of CD4+Ki67+ and CD8+Ki67 + T cells (H andI). Experiments were carried out following the similar protocol as described in (C).

Bars represent mean ± SEM of normalized cell percentages (n = 3∼4 per condition). The experiments were replicated for 3 times. The significance of differences between control group and A53T group was calculated by unpaired Student's t test: $^{**}p < 0.01$, $^{***}p < 0.001$, and $^{****}p < 0.0001$.

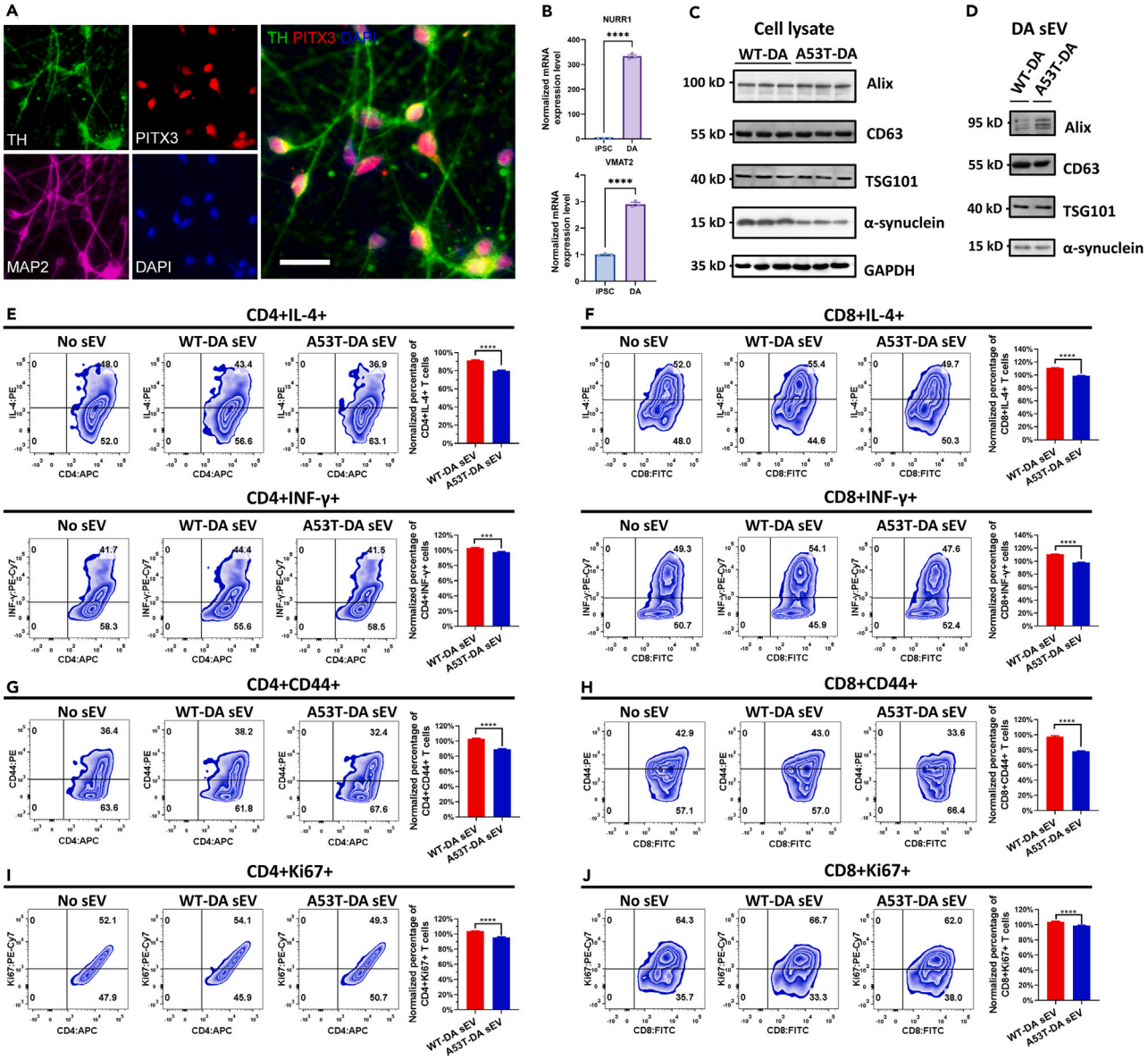

Figure 2. sEVs isolated from DAergic neurons differentiated from human iPSCs with A53T-syn mutation suppress T cells

(A) Representative images of iPSC-derived DA neurons expressing pan-neuronal marker microtubule-associated protein 2 (MAP2) and DA-specific markers TH and PITX3. Scale bars, 20 μm.

(B) RT-qPCR of DA-specific markers *NURR1* and *VMAT2* mRNA expression in iPSCs and iPSC-derived DA neurons. Data are presented as mean ± SEM (n = 3 cultures; ****$p < 0.0001$, unpaired Student's t test).

(C and D) The expressions of sEV/exosome markers and α-synuclein in total cellular lysates (C) and purified sEVs (D) of DAergic neurons differentiated from iPSC. The raw data for all blots were shown in Data S5 and S6.

(E and F) A53T-DA sEV reduces the percentages of INF-γ+ and IL-4+ T cells in both $CD4^+$ (E) and $CD8^+$ (F) T cells. $CD4^+$ or $CD8^+$ T cells isolated from mouse spleens were treated with or without sEVs (10 μg/mL; A53T-DA sEV and WT-DA sEV were prepared from DAergic neurons differentiated from human iPSCs with A53T-syn mutation and isogenic control, respectively) for 48 h. The percentages of cells expressing IL-4 or INF-γ were determined by flow cytometry.

(G–J) A53T-DA sEV reduces the percentages of $CD4^+$ $CD44^+$ (G), $CD8^+CD44^+$ (H), CD4+Ki67+ (I), and CD8+Ki67+ (J) T cells. Experiments were carried out using similar protocols as described in (E).

Bars represent mean ± SEM of normalized cell percentages (n = 4 per condition). The experiments were replicated for 3 times. The significance of differences between control group and A53T group was calculated by unpaired Student's t test: ***$p < 0.001$ and ****$p < 0.0001$.

A53T-syn sEVs suppresses the differentiation of CD4$^+$ T cells into Th1 and Th2 lineages

Because of the general inhibitory effects of A53T-syn sEVs on T cells, we assessed the key transcription factors that are known to control the differentiation of CD4$^+$ T cells. We examined whether Th1-promoting transcription factor T-bet and Th2-promoting transcription factor GATA-3 were altered by A53T-syn sEVs in purified CD4$^+$ T cells. This analysis showed that A53T-syn sEVs isolated from culture media of SN4741 or H4 cells significantly reduced the percentages of CD4+T-bet+ and CD4+GATA-3+ T cells compared to control sEVs (Figures S5A and S5B). Similarly, plasma A53T-NEEVs and A53T-DA sEVs also decreased the percentages of CD4+T-bet+ and CD4+GATA-3+ T cells (Figures S5C and S5D).

To further establish whether A53T-syn sEVs modulated T cell differentiation, we tested the effects of A53T-syn sEVs on murine naive CD4$^+$ T cells under Th0, Th1, and Th2 conditions. Under Th0 condition, we found that plasma A53T-NEEVs significantly reduced the percentages of CD4+IL-4+ and CD4+INF-γ+ T cells (Figure 3A), suggesting an inhibition of differentiation into both Th1 and Th2 lineages. Furthermore, we showed that plasma A53T-NEEVs reduced the differentiation of naive CD4$^+$ T cells into either Th1 or Th2 T cells under their respective conditions (Figures 3B and 3C). Similar to plasma A53T-NEEVs, our analysis showed that A53T-DA sEVs and A53T-syn sEVs from SN4741 cells exhibited similar inhibitory effects on the differentiation of naive CD4$^+$ T cells under Th0, Th1, and Th2 conditions (Figures 3D–3F and S6A–S6C). As shown in Figure S7, the suppression of Th1 and Th2 differentiation by plasma A53T-NEEVs and A53T-DA sEVs was also accompanied by a significant reduction of CD4+T-bet+ and CD4+GATA-3+ T cells under Th0, Th1, and Th2 conditions (Figures S7A–S7H). Therefore, A53T-syn sEV represses the differentiation of naive CD4$^+$ T cells into either Th1 or Th2 lineage.

A53T-syn sEV increases the level of PD-L1 in T cells

Previous studies have shown that tumor-derived exosomes containing PD-L1 significantly suppress CD8$^+$ T cells, leading to the impairment of antitumor immunity in cancer patients.[22] We, therefore, assessed the level of PD-L1 on sEVs/exosomes. Compared to control sEV, we found no significant change in PD-L1 level associated with A53T-syn sEV prepared from culture media of SN4741 cells, plasma of mice, and iPSC-derived DA neurons (Figures S8A–S8E and Data S7 and S8), indicating that the suppressed T cell phenotype induced by A53T-syn sEV is not caused directly by a change of PD-L1 on sEV. We then examined whether A53T-syn sEV affected PD-L1 in T cells and found that exposure of purified CD4$^+$ or CD8$^+$ T cells to A53T-syn sEV isolated from SN4741 and H4 cells, plasma of mice, or iPSC-derived DA neurons all significantly increased the percentages of CD4+PD-L1+ and CD8+PD-L1+ T cells (Figures 4A–4D). More importantly, we found that A53T-syn sEV from SN4741 cells and plasma A53T-NEEVs significantly reduced PD-1+IL-4+, PD-1+INF-γ+, PD-1+T-bet+, and PD-1+GATA-3+ cell percentages in both CD4$^+$ and CD8$^+$ T cells (Figures S9A–S9D). These results suggest that A53T-syn sEV induces PD-L1 on T cells, which correlates with a general suppression of PD-1+ T cells.

Blocking of PD-L1 reverses T cell suppression induced by A53T-syn sEVs

To demonstrate whether PD-L1 was causally associated with T cell suppression induced by A53T-syn sEV, we inhibited PD-L1 and PD-1 binding in T cells with BMS-1166, a small molecule inhibitor of PD-L1.[43] This analysis showed that BMS-1166 significantly reversed the inhibitory effects of A53T-syn sEV from SN4741 cells and plasma A53T-NEEVs on CD4+IL-4+, CD4+INF-γ+, CD8+IL-4+, and CD8+INF-γ+ T cells (Figures 5A–5H). To strengthen the results of PD-L1 inhibitor study, we blocked PD-L1 in T cell cultures using an anti-PD-L1 antibody reported to inhibit PD-L1/PD-1 signaling.[44] This analysis showed that addition of the anti-PD-L1 antibody (4 μg/mL) significantly reversed the suppression of CD4+IL-4+, CD4+INF-γ+, CD8+IL-4+, and CD8+INF-γ+ T cells induced by either A53T-syn sEV isolated from SN4741 cells (Figures S10A–S10D) or plasma A53T-NEEVs (Figures S10E–S10H). Our findings demonstrate that blocking of PD-L1 rescues T cell suppression induced by A53T-syn sEV.

DISCUSSION

Our findings in this study reveal that sEVs isolated from *in vitro* and *in vivo* PD models cause a broad suppression of T cells. This inhibition involves PD-L1 pathway. We show that sEVs isolated from multiple A53T-syn models including SN4741 cells expressing A53T mutant, plasma of A53T-syn transgenic mice, and DAergic neurons derived from human iPSC carrying A53T mutation all suppress the cytokine production by CD4$^+$ and CD8$^+$ T cells. At cellular level, A53T-syn sEV exerts this general suppression, in part, by inhibiting Th1 and Th2 differentiation of naive CD4$^+$ T cells. Furthermore, molecularly, A53T-syn sEV induces the expression of PD-L1 on T cells and PD-L1/PD-1 signaling is required to mediate T cell suppression. These findings highlight the role of PD-associated sEV in the broad dysregulation of T cells in the disease and offer a mechanistic basis for exploring peripheral T cells as biomarkers and therapeutic targets for PD.

Previous studies have shown that the NEEVs from PD patients carry pathological proteins, such as α-synuclein and tau.[24,33,34,45,46] Moreover, α-synuclein and tau proteins in sEV derived from PD patients have been proposed as potential biomarkers for clinical diagnosis and prediction of disease progression.[28,32,34,45–47] However, the immune regulatory role of NEEVs in neurodegenerative diseases has not been defined. Although the PD-derived sEVs containing α-synuclein have been reported to activate peripheral monocytes,[48] the effects of NEEVs on peripheral T cells in neurodegeneration have not been investigated and remained completely undefined. Our current investigation reveals that NEEVs from A53T-syn models exert a strikingly broad suppressive effect on the proliferation, differentiation, activation, and cytokine production of T cells. Collectively, these effects should direct T cells away from an activated pro-inflammatory phenotype in general. Our findings provide a mechanistic explanation for the phenotype of the heterogeneity and reduced T cells in peripheral immune phenotypes in PD reported by multiple studies. For example, it has been shown that peripheral CD3$^+$ T cells are significantly reduced and inactivated while

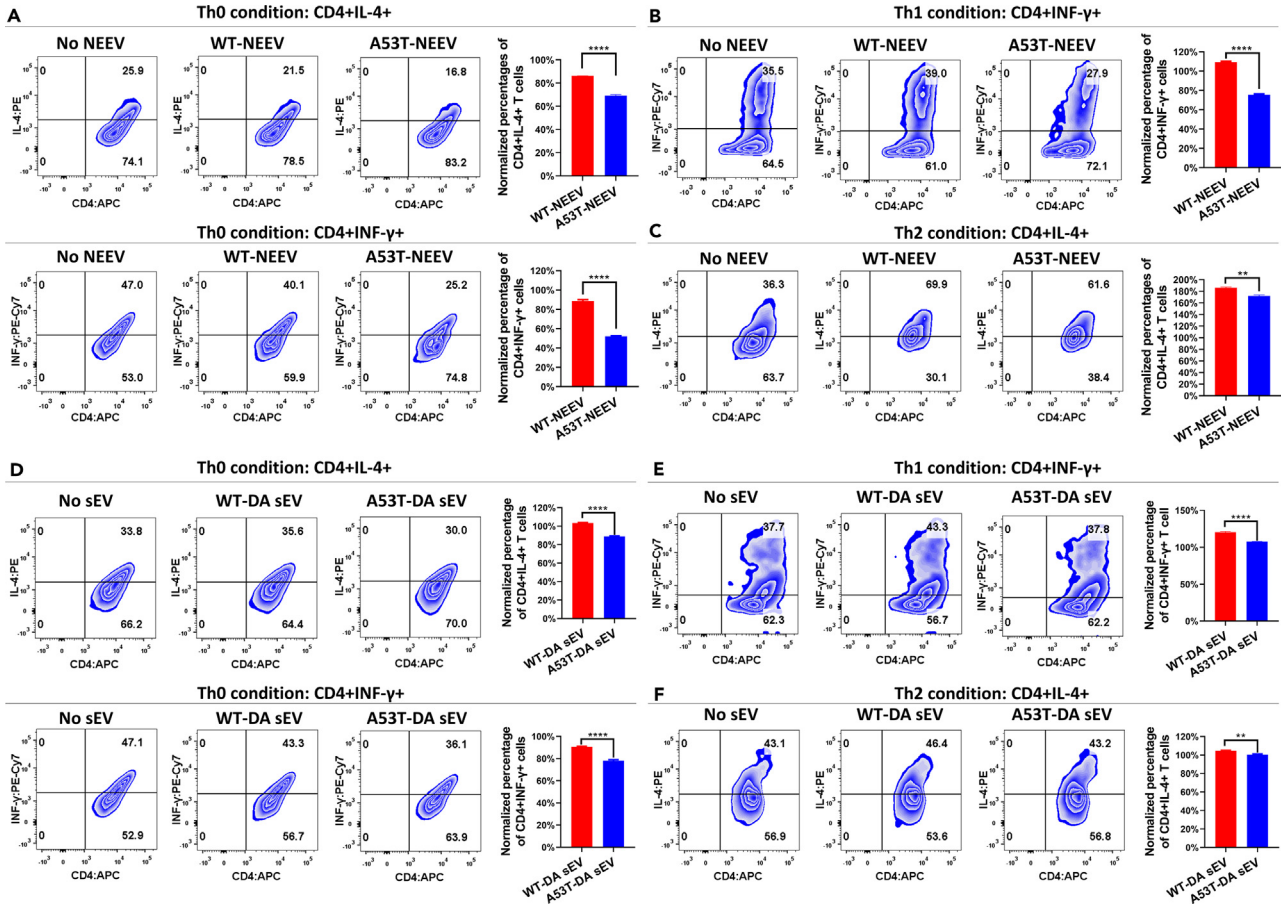

Figure 3. NEEVs isolated from the plasma of A53T-syn transgenic mice and culture media of human iPSC-derived A53T-DA neurons inhibit Th1 and Th2 differentiation

(A) A53T-syn NEEV reduces the percentages of CD4+IL-4+ and CD4+INF-γ+ T cells under Th0 conditions. Naive $CD4^+$ T cells isolated from mouse spleens were treated with or without sEVs (10 μg/mL; WT-NEEV and A53T-NEEV were purified from the plasma of WT mice or A53T α-synuclein transgenic mice, respectively) for 96 h. The percentages of cells expressing IL-4 or INF-γ were determined by flow cytometry.

(B and C) A53T-syn NEEV reduces the percentages of $CD4^+$ T cells with differentiated Th1 or Th2 markers (INF-γ and IL-4, respectively) under either Th1 or Th2 differentiation condition. Naive $CD4^+$ T cells were cultured under Th1 (50 ng/mL recombinant IL-12 and 10 mg/mL anti-IL-4) or Th2 (50 ng/mL recombinant IL-4 and 10 mg/mL anti-IFN-γ) conditions for 24 h. Then cells were treated with or without sEVs (10 μg/mL; WT-NEEV and A53T-NEEV were purified from the plasma of WT mice or A53T α-synuclein transgenic mice, respectively) for 96 h. The percentages of cells expressing IL-4 or INF-γ were determined by flow cytometry.

(D) A53T-DA sEV reduces the percentages of CD4+IL-4+ T cell and CD4+INF-γ+ T cells under Th0 conditions. Experiments were carried out using similar protocols as described in (A) except for the source of sEVs.

(E and F) A53T-DA sEV reduces Th1 and Th2 differentiation under Th1 (E) and Th2 (F) condition. Experiments were carried out using similar protocols as described in (B and C) except for the source of sEVs.

Bars represent mean ± SEM of normalized cell percentages ($n = 4$ per condition). The experiments were replicated for 3 times. The significance of difference between control group and A53T group was calculated by unpaired Student's t test: $^{**}p < 0.01$, $^{***}p < 0.001$, and $^{****}p < 0.0001$.

neutrophils, NK cells, and monocytes are abnormally increased and activated in PD patients.[5–8,10,11,48–50] Our results that NEEVs from multiple A53T-syn models reduce cytokines production by both purified $CD4^+$ and $CD8^+$ T cells are especially interesting in light of the report that the plasma levels of IL-4 and INF-γ in PD patients are reduced.[11] Furthermore, the broad suppressive effects of NEEVs are completely consistent with the reported dysregulation of multiple subtypes of T cells in PD. For example, our finding that activation of purified $CD4^+$ T cells is significantly reduced by NEEVs from A53T-syn models may offer a mechanism underlying disease progression since a reduction of activated $CD4^+$ T cells has been associated with the advancement of PD.[10,11,50] Our finding that A53T-syn sEV suppresses both naive and matured $CD8^+$ T cells supports previous studies reporting decreases of naive $CD8^+$ T cells and cytotoxic $CD8^+$ T cells in PD.[9,50,51] Several studies have noted a decrease of Th1 cells and Th1-promoting transcription factors including *T-bet*, *STAT3*, and *STAT4* in PD patients,[14,52] which is consistent with our finding that A53T-syn NEEVs reduce T-bet level and suppress Th1 differentiation. Thus, the effects of A53T-syn NEEVs identified in the current study explain multiple deficiencies of T cells observed in PD patients.

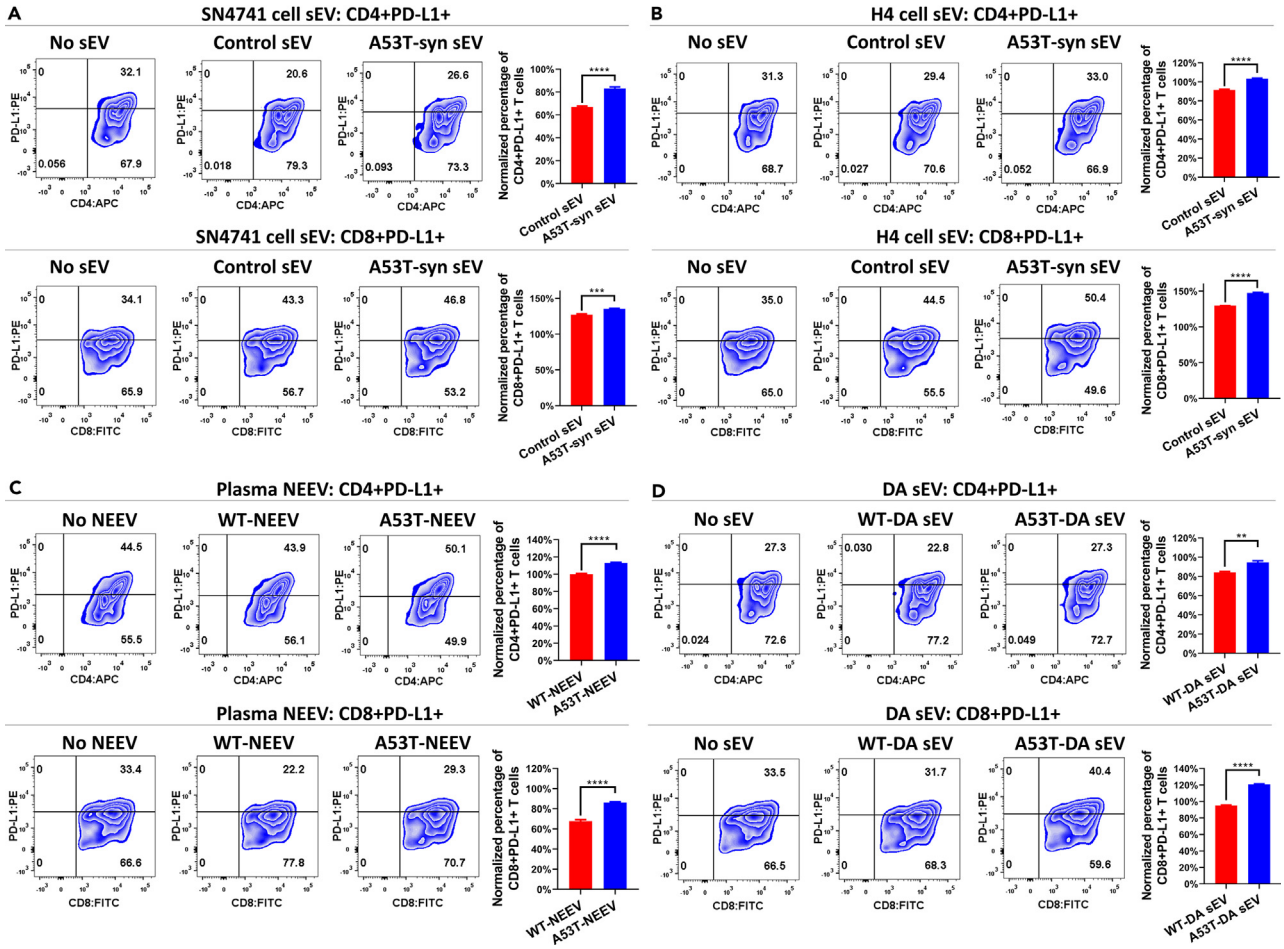

Figure 4. A53T-syn sEVs increase the expression of PD-L1 in CD4$^+$ and CD8$^+$ T cells

(A and B) A53T-syn sEVs from culture media of SN4741 (A) and H4 (B) cells increase the percentages of CD4+PD-L1+ and CD8+PD-L1+ T cells. Purified CD4$^+$ or CD8$^+$ T cells isolated from mouse spleens were treated with or without sEVs (10 μg/mL; control sEV and A53T-syn sEV were prepared from cells without or with A53T α-synuclein overexpression, respectively) for 48 h. The percentages of cells expressing PD-L1 were determined by flow cytometry.

(C and D) A53T-NEEV from A53T-syn transgenic mice (C) or A53T-DA sEV from human iPSC-derived DA neurons (D) increases the percentages of CD4+PD-L1+ and CD8+PD-L1+ T cells. Experiments were carried out using similar protocols as described in (A) except for the source of sEVs.

Bars represent mean ± SEM of normalized cell percentages (n = 4 per condition). The experiments were replicated for 3 times. The significance of differences between control group and A53T group was calculated by unpaired Student's t test: $^{**}p < 0.01$, $^{***}p < 0.001$, and $^{****}p < 0.0001$.

L1CAM, known to regulate neuronal migration and differentiation,[53] is present in NEEVs[33,54] and has been most widely used to extract sEVs of putative neuronal origin for biomarker discovery.[55] In the past decade, anti-L1CAM antibody has been frequently applied to enrich sEVs of neuronal source.[33,35,46,56,57] However, L1CAM is also expressed in non-neural tissues, such as the kidney and gut (https://gtexportal.org/home/gene/L1CAM). Thus, it is possible that L1-positive sEVs are also secreted from other peripheral cell types although direct evidence for this is still lacking. Compared to total plasma sEVs, plasma L1-positive sEVs exhibit higher concentrations of several neuronal markers, such as phosphorylated tau, neuron-specific enolase, MAP2, and neurofilament light chain, highly suggesting at least the enrichment of NEEVs.[54] Considering that the suitability of L1CAM as a specific marker for neuronal sEVs remains to be further clarified, there is a need to develop alternative markers specific for neuron-derived sEVs.

Our studies did not directly address the question if the sex of sEV source may influence its effects. Both ND50085 (A53T mutation-corrected) and ND50086 (A53T mutant) are female iPSC lines (https://stemcells.nindsgenetics.org/) while H4 cell is a male line (https://www.cellosaurus.org/CVCL_1239). But the sex of SN4741 cells and HMC3 cells is unspecified. Since SN4741 cell line is our primary model, we determined the sex of SN4741 cells as male based on the expression of a male-specific genetic marker *SRY* as previously described (Figure S11).[58,59] Given that sEVs used in the study were derived from both male and female cells, our findings are consistent with the interpretation that the effects on T cells exerted by A53T-syn sEVs are not affected by the sex of sEV source. Even though our animal studies were not specifically designed to test the effects of sex of either the source or recipient T cells, the plasma and T cells were obtained from both male and female mice. But fully addressing the role of sex in sEV mediated T cell suppression requires further study.

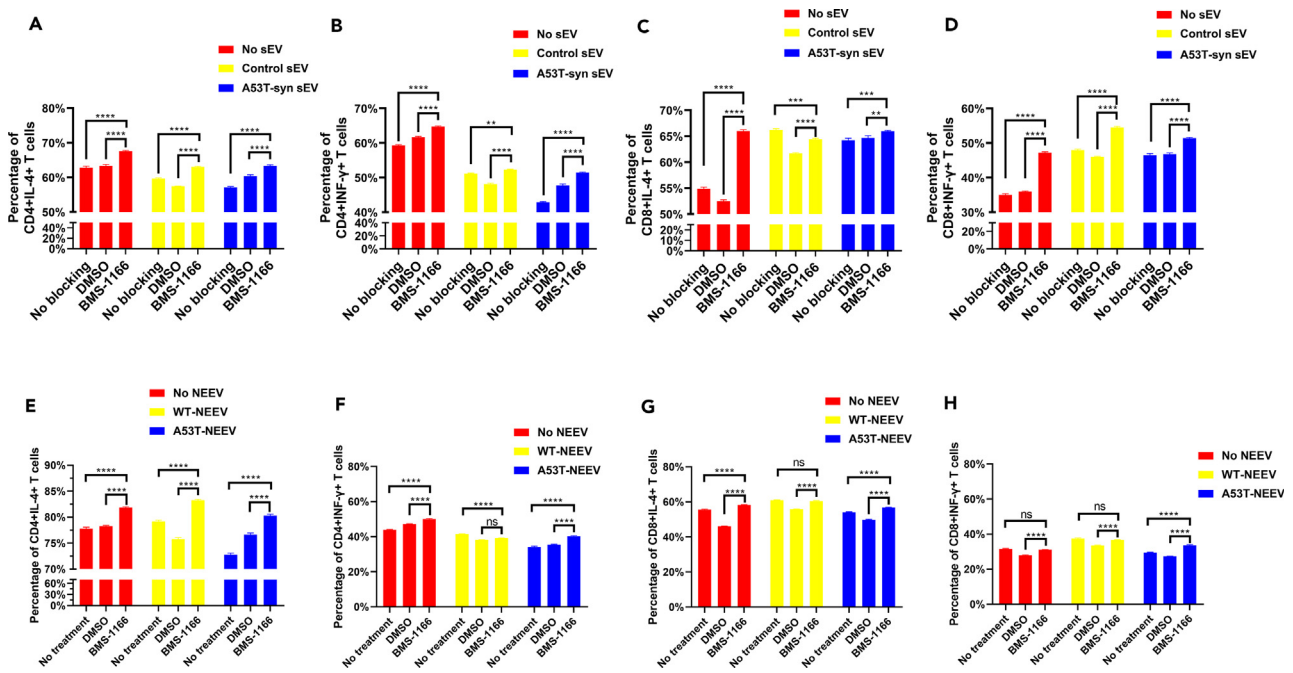

Figure 5. Blocking of PD-L1 with BMS-1166 reverses the immune suppression induced by A53T-syn sEVs

(A–H) Blocking of PD-L1 with BMS-1166 reverses the suppression of IL-4 and INF-γ in $CD4^+$ (A, B, E, and F) or $CD8^+$ (C, D, G, and H) T cells induced by A53T-syn sEV from SN4741 cells (A–D) or by the plasma NEEVs from A53T-syn transgenic mice (E–H). Purified $CD4^+$ or $CD8^+$ T cells isolated from mouse spleens were treated with or without sEVs (10 μg/mL; control sEV and A53T-syn sEV were prepared from cells without or with A53T α-synuclein overexpression, respectively. WT-NEEV and A53T-NEEV were purified from the plasma of WT mice or A53T α-synuclein transgenic mice, respectively) for 48 h. BMS-1166 (1 μM for final concertation) was added to the $CD4^+$ and $CD8^+$ T cell culture media before the treatment of sEVs. The percentages of cells expressing IL-4 or INF-γ were determined by flow cytometry.

Bars represent mean ± SEM of cell percentages ($n = 4$ per condition). The experiments were replicated for 3 times. The significance of differences among three groups was assessed by two-way ANOVA followed by Tukey's multiple comparisons test: $^{**}p < 0.01$, $^{***}p < 0.001$, and $^{****}p < 0.0001$.

The primary model used in our study is sEV derived from A53T-syn conditions. Previous studies have revealed that the expression of leucine-rich repeat kinase 2 (LRRK2) was increased in T cells[60] and G2019S *LRRK2* mutant significantly suppresses Th17 cell differentiation,[61] indicating that *LRRK2* (G2019S) also regulates T cell immunity. The *LRRK2* G2019S mutation has also been shown to alter astrocyte-to-neuron communication via extracellular vesicles.[62] In addition, *LRRK2* mutation can alter sEVs/exosome contents.[62] Furthermore, the mutations of *GBA* (glucocerebrosidase) and *ATP13A2* have been reported to increase α-synuclein secretion through exosomes.[63,64] Together with these findings, our results raise the possibility that sEVs/exosomes derived from neural cells may be involved in regulating T cells under a broad range of pathogenic conditions associated with mutations in *SNCA*, *LRRK2*, *GBA*, or *ATP13A2* in PD.

Accumulating evidence has shown that sEVs/exosomes containing PD-L1 released by cancer cells inhibit anti-tumor immunity and blocking PD-1 or PD-L1 provides therapeutic benefits for multiple types of cancers.[22,23,65–68] But the role of sEVs/exosomes-mediated regulation of immune checkpoint in neurodegenerative diseases remains poorly understood. We found no significant change of PD-L1 in A53T-syn sEV compared to control sEV. Thus, the level of PD-L1 on sEV does not appear to explain the T cell immunosuppression induced by A53T-syn sEV. Instead, our data show that exposure to A53T-syn sEV increases the expression of PD-L1 in T cells. This is consistent with several studies showing that tumor-derived exosomes modulate PD-L1 levels in immune cells.[31,69] Since inhibiting PD-L1 by either an antibody or the small molecule inhibitor BMS-1166 can alleviate the inhibitory effects of NEEVs on T cells in our experimental paradigms, it supports a model in which PD-L1/PD-1 expressed by T cells mediates NEEV-induced suppression of T cell immunity in PD. This is clinically significant, considering that low lymphocyte count is associated with increased PD risk and worse disease progression.[3,4,6,7,52] The regulation of T cell profiles with sargramostim (granulocyte-macrophage colony-stimulating factor) has been shown to improve motor functions in PD patients.[70,71] Whether PD-1/PD-L1 blockade alone is sufficient to alter the pathology and affect cognition in mouse models of AD or related diseases remains to be clarified.[72–75] Our findings clearly highlight the possibility of inhibiting PD-L1/PD-1 pathway as a therapeutical strategy to alleviate broad T cell deficiency and potentially disease progression in PD. Interestingly, PD-1 deficiency has been shown to aggravate motor dysfunction in MTPT model of PD.[76] Thus, the role of PD-L1/PD-1 axis in the pathogenesis and treatment of PD requires further assessment.

Although we showed that A53T-syn sEV induces T cell suppression in a PD-1/PD-L1 dependent manner. The molecular mechanisms underlying the increase of PD-L1 in T cells induced by A53T-syn sEV need further investigation. The expression of PD-L1 is controlled by multiple mechanisms.[77] For example, cytokines, microRNAs, and noncoding Y RNA contained in sEVs/exosomes have been shown to increase PD-L1

expression in immune cells.[31,78–80] NEEVs extracted from plasma or cerebrospinal fluid of PD patients are shown to contain various pathogenic proteins.[24,33,34,45,46] Given our finding that NEEVs regulate T cell immunity, one important future direction is to decipher the components in A53T-syn sEV and signaling events trigged in T cells responsible for regulating T cell PD-L1 expression and subsequent responses.

Limitations of the study

One of the limitations of the study is the lack of *in vivo* data demonstrating the effects of NEEVs on peripheral blood T cells in the context of PD. In addition, we did not decode the molecular components of NEEVs mediating the suppressive phenotypes of T cells. Furthermore, our investigation did not address fully whether sex of the recipient T cells may affect their response to sEVs. They should be addressed by future studies.

STAR★METHODS

Detailed methods are provided in the online version of this paper and include the following:

- KEY RESOURCES TABLE
- RESOURCE AVAILABILITY
  - Lead contact
  - Materials availability
  - Data and code availability
- EXPERIMENTAL MODEL AND STUDY PARTICIPANT DETAILS
  - Mice
- METHOD DETAILS
  - Cell lines
  - Reagents
  - Transfection
  - DAergic neurons culture
  - sEV extraction from cell culture medium
  - NEEVs extraction from mouse plasma
  - Nanoparticle tracking analysis
  - Western blot
  - Transmission electron microscopy
  - Isolation of mouse spleen cells, $CD4^+$ T cells, and $CD8^+$ T cells
  - Culture of mouse spleen cells, $CD4^+$ T cells, and $CD8^+$ T cells
  - Differentiation induction of mouse naive $CD4^+$ T cells
  - sEVs labeling and internalization
  - sEVs treatment
  - Blocking of PD-L1
  - Flow cytometry
  - Immunocytochemistry
  - RNA isolation, RT-PCR, and RT-qPCR
- QUANTIFICATIONS AND STATISTICAL ANALYSIS
  - Statistical analyses

SUPPLEMENTAL INFORMATION

Supplemental information can be found online at https://doi.org/10.1016/j.isci.2024.110243.

ACKNOWLEDGMENTS

This work was supported in part by grant 1RF1AG069253-01A1 (Z.M).

AUTHOR CONTRIBUTIONS

Z.C.: formal analysis, investigation, methodology, figure preparation, and writing – review and editing; W.L., B.M., C.X., and Y.H.: formal analysis, investigation, methodology; G.L.: formal analysis, data curation, and investigation; Z.W.: supervision, validation, investigation, and methodology; J.L.: conceptualization, supervision, writing – original draft, review and editing; Z.M.: conceptualization, formal analysis, supervision, funding acquisition, project administration, investigation, methodology, writing – original draft, and review and editing.

DECLARATION OF INTERESTS

The authors declare no competing interests.

Received: January 23, 2024
Revised: April 16, 2024
Accepted: June 7, 2024
Published: June 11, 2024

REFERENCES

1. Contaldi, E., Magistrelli, L., and Comi, C. (2022). T Lymphocytes in Parkinson's Disease. J. Parkinsons Dis. *12*, S65–S74. https://doi.org/10.3233/JPD-223152.
2. Chen, Z., Chen, S., and Liu, J. (2018). The role of T cells in the pathogenesis of Parkinson's disease. Prog. Neurobiol. *169*, 1–23. https://doi.org/10.1016/j.pneurobio.2018.08.002.
3. Yazdani, S., Mariosa, D., Hammar, N., Andersson, J., Ingre, C., Walldius, G., and Fang, F. (2019). Peripheral immune biomarkers and neurodegenerative diseases: A prospective cohort study with 20 years of follow-up. Ann. Neurol. *86*, 913–926. https://doi.org/10.1002/ana.25614.
4. Jensen, M.P., Jacobs, B.M., Dobson, R., Bandres-Ciga, S., Blauwendraat, C., Schrag, A., and Noyce, A.J.; International Parkinson's Disease Genomics Consortium IPDGC (2021). Lower Lymphocyte Count is Associated With Increased Risk of Parkinson's Disease. Ann. Neurol. *89*, 803–812. https://doi.org/10.1002/ana.26034.
5. Stevens, C.H., Rowe, D., Morel-Kopp, M.C., Orr, C., Russell, T., Ranola, M., Ward, C., and Halliday, G.M. (2012). Reduced T helper and B lymphocytes in Parkinson's disease. J. Neuroimmunol. *252*, 95–99. https://doi.org/10.1016/j.jneuroim.2012.07.015.
6. Jin, H., Gu, H.Y., Mao, C.J., Chen, J., and Liu, C.F. (2020). Association of inflammatory factors and aging in Parkinson's disease. Neurosci. Lett. *736*, 135259. https://doi.org/10.1016/j.neulet.2020.135259.
7. Sun, C., Zhao, Z., Yu, W., Mo, M., Song, C., Si, Y., and Liu, Y. (2019). Abnormal subpopulations of peripheral blood lymphocytes are involved in Parkinson's disease. Ann. Transl. Med. *7*, 637. https://doi.org/10.21037/atm.2019.10.105.
8. Cen, L., Yang, C., Huang, S., Zhou, M., Tang, X., Li, K., Guo, W., Wu, Z., Mo, M., Xiao, Y., et al. (2017). Peripheral Lymphocyte Subsets as a Marker of Parkinson's Disease in a Chinese Population. Neurosci. Bull. *33*, 493–500. https://doi.org/10.1007/s12264-017-0163-9.
9. Bhatia, D., Grozdanov, V., Ruf, W.P., Kassubek, J., Ludolph, A.C., Weishaupt, J.H., and Danzer, K.M. (2021). T-cell dysregulation is associated with disease severity in Parkinson's Disease. J. Neuroinflammation *18*, 250. https://doi.org/10.1186/s12974-021-02296-8.
10. Garfias, S., Tamaya Dominguez, B., Toledo Rojas, A., Arroyo, M., Rodriguez, U., Boll, C., Sosa, A.L., Sciutto, E., Adalid-Peralta, L., Martinez Lopez, Y., et al. (2022). Peripheral blood lymphocyte phenotypes in Alzheimer and Parkinson's diseases. Neurologia *37*, 110–121. https://doi.org/10.1016/j.nrl.2018.10.004.
11. Rocha, N.P., Assis, F., Scalzo, P.L., Vieira, É.L.M., Barbosa, I.G., de Souza, M.S., Christo, P.P., Reis, H.J., and Teixeira, A.L. (2018). Reduced Activated T Lymphocytes (CD4+CD25+) and Plasma Levels of Cytokines in Parkinson's Disease. Mol. Neurobiol. *55*, 1488–1497. https://doi.org/10.1007/s12035-017-0404-y.
12. Yan, Z., Yang, W., Wei, H., Dean, M.N., Standaert, D.G., Cutter, G.R., Benveniste, E.N., and Qin, H. (2021). Dysregulation of the Adaptive Immune System in Patients With Early-Stage Parkinson Disease. Neurol. Neuroimmunol. Neuroinflamm. *8*, e1036. https://doi.org/10.1212/NXI.0000000000001036.
13. Alvarez-Luquin, D.D., Arce-Sillas, A., Leyva-Hernandez, J., Sevilla-Reyes, E., Boll, M.C., Montes-Moratilla, E., Vivas-Almazan, V., Perez-Correa, C., Rodriguez-Ortiz, U., Espinoza-Cardenas, R., et al. (2019). Regulatory impairment in untreated Parkinson's disease is not restricted to Tregs: other regulatory populations are also involved. J. Neuroinflammation *16*, 212. https://doi.org/10.1186/s12974-019-1606-1.
14. De Francesco, E., Terzaghi, M., Storelli, E., Magistrelli, L., Comi, C., Legnaro, M., Mauri, M., Marino, F., Versino, M., and Cosentino, M. (2021). CD4+ T-Cell Transcription Factors in Idiopathic REM Sleep Behavior Disorder and Parkinson's Disease. Mov. Disord. *36*, 225–229. https://doi.org/10.1002/mds.28137.
15. Brochard, V., Combadière, B., Prigent, A., Laouar, Y., Perrin, A., Beray-Berthat, V., Bonduelle, O., Alvarez-Fischer, D., Callebert, J., Launay, J.M., et al. (2009). Infiltration of CD4+ lymphocytes into the brain contributes to neurodegeneration in a mouse model of Parkinson disease. J. Clin. Invest. *119*, 182–192. https://doi.org/10.1172/JCI36470.
16. Cebrian, C., Zucca, F.A., Mauri, P., Steinbeck, J.A., Studer, L., Scherzer, C.R., Kanter, E., Budhu, S., Mandelbaum, J., Vonsattel, J.P., et al. (2014). MHC-I expression renders catecholaminergic neurons susceptible to T-cell-mediated degeneration. Nat. Commun. *5*, 3633. https://doi.org/10.1038/ncomms4633.
17. Williams, G.P., Schonhoff, A.M., Jurkuvenaite, A., Gallups, N.J., Standaert, D.G., and Harms, A.S. (2021). CD4 T cells mediate brain inflammation and neurodegeneration in a mouse model of Parkinson's disease. Brain *144*, 2047–2059. https://doi.org/10.1093/brain/awab103.
18. Galiano-Landeira, J., Torra, A., Vila, M., and Bové, J. (2020). CD8 T cell nigral infiltration precedes synucleinopathy in early stages of Parkinson's disease. Brain *143*, 3717–3733. https://doi.org/10.1093/brain/awaa269.
19. van Niel, G., D'Angelo, G., and Raposo, G. (2018). Shedding light on the cell biology of extracellular vesicles. Nat. Rev. Mol. Cell Biol. *19*, 213–228. https://doi.org/10.1038/nrm.2017.125.
20. Kalluri, R., and LeBleu, V.S. (2020). The biology, function, and biomedical applications of exosomes. Science *367*, eaau6977. https://doi.org/10.1126/science.aau6977.
21. Nabet, B.Y., Qiu, Y., Shabason, J.E., Wu, T.J., Yoon, T., Kim, B.C., Benci, J.L., DeMichele, A.M., Tchou, J., Marcotrigiano, J., and Minn, A.J. (2017). Exosome RNA Unshielding Couples Stromal Activation to Pattern Recognition Receptor Signaling in Cancer. Cell *170*, 352–366.e13. https://doi.org/10.1016/j.cell.2017.06.031.
22. Chen, G., Huang, A.C., Zhang, W., Zhang, G., Wu, M., Xu, W., Yu, Z., Yang, J., Wang, B., Sun, H., et al. (2018). Exosomal PD-L1 contributes to immunosuppression and is associated with anti-PD-1 response. Nature *560*, 382–386. https://doi.org/10.1038/s41586-018-0392-8.
23. Poggio, M., Hu, T., Pai, C.C., Chu, B., Belair, C.D., Chang, A., Montabana, E., Lang, U.E., Fu, Q., Fong, L., and Blelloch, R. (2019). Suppression of Exosomal PD-L1 Induces Systemic Anti-tumor Immunity and Memory. Cell *177*, 414–427.e13. https://doi.org/10.1016/j.cell.2019.02.016.
24. Fussi, N., Höllerhage, M., Chakroun, T., Nykänen, N.P., Rösler, T.W., Koeglsperger, T., Wurst, W., Behrends, C., and Höglinger, G.U. (2018). Exosomal secretion of alpha-synuclein as protective mechanism after upstream blockage of macroautophagy. Cell Death Dis. *9*, 757. https://doi.org/10.1038/s41419-018-0816-2.
25. Eren, E., Hunt, J.F.V., Shardell, M., Chawla, S., Tran, J., Gu, J., Vogt, N.M., Johnson, S.C., Bendlin, B.B., and Kapogiannis, D. (2020). Extracellular vesicle biomarkers of Alzheimer's disease associated with sub-clinical cognitive decline in late middle age. Alzheimers Dement. *16*, 1293–1304. https://doi.org/10.1002/alz.12130.
26. Asai, H., Ikezu, S., Tsunoda, S., Medalla, M., Luebke, J., Haydar, T., Wolozin, B., Butovsky, O., Kügler, S., and Ikezu, T. (2015). Depletion of microglia and inhibition of exosome synthesis halt tau propagation. Nat. Neurosci. *18*, 1584–1593. https://doi.org/10.1038/nn.4132.
27. Feiler, M.S., Strobel, B., Freischmidt, A., Helferich, A.M., Kappel, J., Brewer, B.M., Li, D., Thal, D.R., Walther, P., Ludolph, A.C., et al. (2015). TDP-43 is intercellularly transmitted across axon terminals. J. Cell Biol. *211*, 897–911. https://doi.org/10.1083/jcb.201504057.
28. Minakaki, G., Menges, S., Kittel, A., Emmanouilidou, E., Schaeffner, I., Barkovits, K., Bergmann, A., Rockenstein, E., Adame, A., Marxreiter, F., et al. (2018). Autophagy inhibition promotes SNCA/alpha-synuclein release and transfer via extracellular vesicles with a hybrid autophagosome-exosome-like phenotype. Autophagy *14*, 98–119. https://doi.org/10.1080/15548627.2017.1395992.
29. Stuendl, A., Kunadt, M., Kruse, N., Bartels, C., Moebius, W., Danzer, K.M., Mollenhauer, B., and Schneider, A. (2016). Induction of alpha-synuclein aggregate formation by CSF exosomes from patients with Parkinson's disease and dementia with Lewy bodies. Brain *139*, 481–494. https://doi.org/10.1093/brain/awv346.
30. Dinkins, M.B., Dasgupta, S., Wang, G., Zhu, G., and Bieberich, E. (2014). Exosome reduction in vivo is associated with lower amyloid plaque load in the 5XFAD mouse model of Alzheimer's disease. Neurobiol.

Aging *35*, 1792–1800. https://doi.org/10.1016/j.neurobiolaging.2014.02.012.

31. Yao, X., Tu, Y., Xu, Y., Guo, Y., Yao, F., and Zhang, X. (2020). Endoplasmic reticulum stress-induced exosomal miR-27a-3p promotes immune escape in breast cancer via regulating PD-L1 expression in macrophages. J. Cell Mol. Med. *24*, 9560–9573. https://doi.org/10.1111/jcmm.15367.
32. Jiang, C., Hopfner, F., Berg, D., Hu, M.T., Pilotto, A., Borroni, B., Davis, J.J., and Tofaris, G.K. (2021). Validation of alpha-Synuclein in L1CAM-Immunocaptured Exosomes as a Biomarker for the Stratification of Parkinsonian Syndromes. Mov. Disord. *36*, 2663–2669. https://doi.org/10.1002/mds.28591.
33. Shi, M., Liu, C., Cook, T.J., Bullock, K.M., Zhao, Y., Ginghina, C., Li, Y., Aro, P., Dator, R., He, C., et al. (2014). Plasma exosomal alpha-synuclein is likely CNS-derived and increased in Parkinson's disease. Acta Neuropathol. *128*, 639–650. https://doi.org/10.1007/s00401-014-1314-y.
34. Niu, M., Li, Y., Li, G., Zhou, L., Luo, N., Yao, M., Kang, W., and Liu, J. (2020). A longitudinal study on alpha-synuclein in plasma neuronal exosomes as a biomarker for Parkinson's disease development and progression. Eur. J. Neurol. *27*, 967–974. https://doi.org/10.1111/ene.14208.
35. Jiang, C., Hopfner, F., Katsikoudi, A., Hein, R., Catli, C., Evetts, S., Huang, Y., Wang, H., Ryder, J.W., Kuhlenbaeumer, G., et al. (2020). Serum neuronal exosomes predict and differentiate Parkinson's disease from atypical parkinsonism. J. Neurol. Neurosurg. Psychiatry *91*, 720–729. https://doi.org/10.1136/jnnp-2019-322588.
36. Zhu, C., Bilousova, T., Focht, S., Jun, M., Elias, C.J., Melnik, M., Chandra, S., Campagna, J., Cohn, W., Hatami, A., et al. (2021). Pharmacological inhibition of nSMase2 reduces brain exosome release and alpha-synuclein pathology in a Parkinson's disease model. Mol. Brain *14*, 70. https://doi.org/10.1186/s13041-021-00776-9.
37. Sulzer, D., Alcalay, R.N., Garretti, F., Cote, L., Kanter, E., Agin-Liebes, J., Liong, C., McMurtrey, C., Hildebrand, W.H., Mao, X., et al. (2017). T cells from patients with Parkinson's disease recognize alpha-synuclein peptides. Nature *546*, 656–661. https://doi.org/10.1038/nature22815.
38. Yang, J., Luo, S., Zhang, J., Yu, T., Fu, Z., Zheng, Y., Xu, X., Liu, C., Fan, M., and Zhang, Z. (2021). Exosome-mediated delivery of antisense oligonucleotides targeting alpha-synuclein ameliorates the pathology in a mouse model of Parkinson's disease. Neurobiol. Dis. *148*, 105218. https://doi.org/10.1016/j.nbd.2020.105218.
39. Garcia-Martin, R., Wang, G., Brandão, B.B., Zanotto, T.M., Shah, S., Kumar Patel, S., Schilling, B., and Kahn, C.R. (2022). MicroRNA sequence codes for small extracellular vesicle release and cellular retention. Nature *601*, 446–451. https://doi.org/10.1038/s41586-021-04234-3.
40. Kurzawa-Akanbi, M., Tammireddy, S., Fabrik, I., Gliaudelytė, L., Doherty, M.K., Heap, R., Matečko-Burmann, I., Burmann, B.M., Trost, M., Lucocq, J.M., et al. (2021). Altered ceramide metabolism is a feature in the extracellular vesicle-mediated spread of alpha-synuclein in Lewy body disorders. Acta Neuropathol. *142*, 961–984. https://doi.org/10.1007/s00401-021-02367-3.
41. Dong, L., Helmke, A., Waisman, A., Haller, H., Pich, A., and von Vietinghoff, S. (2016). Surface-bound bovine serum albumin carrier protein as present in recombinant cytokine preparations amplifies T helper 17 cell polarization. Sci. Rep. *6*, 36598. https://doi.org/10.1038/srep36598.
42. Zhang, C., Zhu, Z., Gao, J., Yang, L., Dang, E., Fang, H., Shao, S., Zhang, S., Xiao, C., Yuan, X., et al. (2020). Plasma exosomal miR-375-3p regulates mitochondria-dependent keratinocyte apoptosis by targeting XIAP in severe drug-induced skin reactions. Sci. Transl. Med. *12*, eaaw6142. https://doi.org/10.1126/scitranslmed.aaw6142.
43. Skalniak, L., Zak, K.M., Guzik, K., Magiera, K., Musielak, B., Pachota, M., Szelazek, B., Kocik, J., Grudnik, P., Tomala, M., et al. (2017). Small-molecule inhibitors of PD-1/PD-L1 immune checkpoint alleviate the PD-L1-induced exhaustion of T-cells. Oncotarget *8*, 72167–72181. https://doi.org/10.18632/oncotarget.20050.
44. Esch, K.J., Juelsgaard, R., Martinez, P.A., Jones, D.E., and Petersen, C.A. (2013). Programmed death 1-mediated T cell exhaustion during visceral leishmaniasis impairs phagocyte function. J. Immunol. *191*, 5542–5550. https://doi.org/10.4049/jimmunol.1301810.
45. Cerri, S., Ghezzi, C., Sampieri, M., Siani, F., Avenali, M., Dornini, G., Zangaglia, R., Minafra, B., and Blandini, F. (2018). The Exosomal/Total alpha-Synuclein Ratio in Plasma Is Associated With Glucocerebrosidase Activity and Correlates With Measures of Disease Severity in PD Patients. Front. Cell. Neurosci. *12*, 125. https://doi.org/10.3389/fncel.2018.00125.
46. Shi, M., Kovac, A., Korff, A., Cook, T.J., Ginghina, C., Bullock, K.M., Yang, L., Stewart, T., Zheng, D., Aro, P., et al. (2016). CNS tau efflux via exosomes is likely increased in Parkinson's disease but not in Alzheimer's disease. Alzheimers Dement. *12*, 1125–1131. https://doi.org/10.1016/j.jalz.2016.04.003.
47. Kluge, A., Bunk, J., Schaeffer, E., Drobny, A., Xiang, W., Knacke, H., Bub, S., Lückstädt, W., Arnold, P., Lucius, R., et al. (2022). Detection of neuron-derived pathological alpha-synuclein in blood. Brain *145*, 3058–3071. https://doi.org/10.1093/brain/awac115.
48. Grozdanov, V., Bousset, L., Hoffmeister, M., Bliederhaeuser, C., Meier, C., Madiona, K., Pieri, L., Kiechle, M., McLean, P.J., Kassubek, J., et al. (2019). Increased Immune Activation by Pathologic alpha-Synuclein in Parkinson's Disease. Ann. Neurol. *86*, 593–606. https://doi.org/10.1002/ana.25557.
49. Grozdanov, V., Bliederhaeuser, C., Ruf, W.P., Roth, V., Fundel-Clemens, K., Zondler, L., Brenner, D., Martin-Villalba, A., Hengerer, B., Kassubek, J., et al. (2014). Inflammatory dysregulation of blood monocytes in Parkinson's disease patients. Acta Neuropathol. *128*, 651–663. https://doi.org/10.1007/s00401-014-1345-4.
50. Jiang, S., Gao, H., Luo, Q., Wang, P., and Yang, X. (2017). The correlation of lymphocyte subsets, natural killer cell, and Parkinson's disease: a meta-analysis. Neurol. Sci. *38*, 1373–1380. https://doi.org/10.1007/s10072-017-2988-4.
51. He, Y., Peng, K., Li, R., Zhang, Z., Pan, L., Zhang, T., Lin, A., Hong, R., Nie, Z., Guan, Q., and Jin, L. (2022). Changes of T lymphocyte subpopulations and their roles in predicting the risk of Parkinson's disease. J. Neurol. *269*, 5368–5381. https://doi.org/10.1007/s00415-022-11190-z.
52. Niwa, F., Kuriyama, N., Nakagawa, M., and Imanishi, J. (2012). Effects of peripheral lymphocyte subpopulations and the clinical correlation with Parkinson's disease. Geriatr. Gerontol. Int. *12*, 102–107. https://doi.org/10.1111/j.1447-0594.2011.00740.x.
53. Maness, P.F., and Schachner, M. (2007). Neural recognition molecules of the immunoglobulin superfamily: signaling transducers of axon guidance and neuronal migration. Nat. Neurosci. *10*, 19–26. https://doi.org/10.1038/nn1827.
54. Mustapic, M., Eitan, E., Werner, J.K., Jr., Berkowitz, S.T., Lazaropoulos, M.P., Tran, J., Goetzl, E.J., and Kapogiannis, D. (2017). Plasma Extracellular Vesicles Enriched for Neuronal Origin: A Potential Window into Brain Pathologic Processes. Front. Neurosci. *11*, 278. https://doi.org/10.3389/fnins.2017.00278.
55. Pulliam, L., Sun, B., Mustapic, M., Chawla, S., and Kapogiannis, D. (2019). Plasma neuronal exosomes serve as biomarkers of cognitive impairment in HIV infection and Alzheimer's disease. J. Neurovirol. *25*, 702–709. https://doi.org/10.1007/s13365-018-0695-4.
56. Athauda, D., Gulyani, S., Karnati, H.K., Li, Y., Tweedie, D., Mustapic, M., Chawla, S., Chowdhury, K., Skene, S.S., Greig, N.H., et al. (2019). Utility of Neuronal-Derived Exosomes to Examine Molecular Mechanisms That Affect Motor Function in Patients With Parkinson Disease: A Secondary Analysis of the Exenatide-PD Trial. JAMA Neurol. *76*, 420–429. https://doi.org/10.1001/jamaneurol.2018.4304.
57. Huang, Y., Liu, Z., Li, N., Tian, C., Yang, H., Huo, Y., Li, Y., Zhang, J., and Yu, Z. (2022). Parkinson's Disease Derived Exosomes Aggravate Neuropathology in SNCA*A53T Mice. Ann. Neurol. *92*, 230–245. https://doi.org/10.1002/ana.26421.
58. Lambert, J.F., Benoit, B.O., Colvin, G.A., Carlson, J., Delville, Y., and Quesenberry, P.J. (2000). Quick sex determination of mouse fetuses. J. Neurosci. Methods *95*, 127–132. https://doi.org/10.1016/s0165-0270(99)00157-0.
59. Deeney, S., Powers, K.N., and Crombleholme, T.M. (2016). A comparison of sexing methods in fetal mice. Lab. Anim *45*, 380–384. https://doi.org/10.1038/laban.1105.
60. Cook, D.A., Kannarkat, G.T., Cintron, A.F., Butkovich, L.M., Fraser, K.B., Chang, J., Grigoryan, N., Factor, S.A., West, A.B., Boss, J.M., and Tansey, M.G. (2017). LRRK2 levels in immune cells are increased in Parkinson's disease. NPJ Parkinsons Dis. *3*, 11. https://doi.org/10.1038/s41531-017-0010-8.
61. Park, J., Lee, J.W., Cooper, S.C., Broxmeyer, H.E., Cannon, J.R., and Kim, C.H. (2017). Parkinson disease-associated LRRK2 G2019S transgene disrupts marrow myelopoiesis and peripheral Th17 response. J. Leukoc. Biol. *102*, 1093–1102. https://doi.org/10.1189/jlb.1A0417-147RR.
62. de Rus Jacquet, A., Tancredi, J.L., Lemire, A.L., DeSantis, M.C., Li, W.P., and O'Shea, E.K. (2021). The LRRK2 G2019S mutation alters astrocyte-to-neuron communication via extracellular vesicles and induces neuron atrophy in a human iPSC-derived model of Parkinson's disease. Elife *10*, e73062. https://doi.org/10.7554/eLife.73062.
63. Papadopoulos, V.E., Nikolopoulou, G., Antoniadou, I., Karachaliou, A., Arianoglou, G., Emmanouilidou, E., Sardi, S.P., Stefanis,

L., and Vekrellis, K. (2018). Modulation of beta-glucocerebrosidase increases alpha-synuclein secretion and exosome release in mouse models of Parkinson's disease. Hum. Mol. Genet. *27*, 1696–1710. https://doi.org/10.1093/hmg/ddy075.

64. Tsunemi, T., Hamada, K., and Krainc, D. (2014). ATP13A2/PARK9 regulates secretion of exosomes and alpha-synuclein. J. Neurosci. *34*, 15281–15287. https://doi.org/10.1523/JNEUROSCI.1629-14.2014.
65. Eroglu, Z., Zaretsky, J.M., Hu-Lieskovan, S., Kim, D.W., Algazi, A., Johnson, D.B., Liniker, E., Ben, K., Munhoz, R., Rapisuwon, S., et al. (2018). High response rate to PD-1 blockade in desmoplastic melanomas. Nature *553*, 347–350. https://doi.org/10.1038/nature25187.
66. Mok, T.S.K., Wu, Y.L., Kudaba, I., Kowalski, D.M., Cho, B.C., Turna, H.Z., Castro, G., Jr., Srimuninnimit, V., Laktionov, K.K., Bondarenko, I., et al. (2019). Pembrolizumab versus chemotherapy for previously untreated, PD-L1-expressing, locally advanced or metastatic non-small-cell lung cancer (KEYNOTE-042): a randomised, open-label, controlled, phase 3 trial. Lancet *393*, 1819–1830. https://doi.org/10.1016/S0140-6736(18)32409-7.
67. Cortes, J., Cescon, D.W., Rugo, H.S., Nowecki, Z., Im, S.A., Yusof, M.M., Gallardo, C., Lipatov, O., Barrios, C.H., Holgado, E., et al. (2020). Pembrolizumab plus chemotherapy versus placebo plus chemotherapy for previously untreated locally recurrent inoperable or metastatic triple-negative breast cancer (KEYNOTE-355): a randomised, placebo-controlled, double-blind, phase 3 clinical trial. Lancet *396*, 1817–1828. https://doi.org/10.1016/S0140-6736(20)32531-9.
68. Janjigian, Y.Y., Shitara, K., Moehler, M., Garrido, M., Salman, P., Shen, L., Wyrwicz, L., Yamaguchi, K., Skoczylas, T., Campos Bragagnoli, A., et al. (2021). First-line nivolumab plus chemotherapy versus chemotherapy alone for advanced gastric, gastro-oesophageal junction, and oesophageal adenocarcinoma (CheckMate 649): a randomised, open-label, phase 3 trial. Lancet *398*, 27–40. https://doi.org/10.1016/S0140-6736(21)00797-2.
69. Gabrusiewicz, K., Li, X., Wei, J., Hashimoto, Y., Marisetty, A.L., Ott, M., Wang, F., Hawke, D., Yu, J., Healy, L.M., et al. (2018). Glioblastoma stem cell-derived exosomes induce M2 macrophages and PD-L1 expression on human monocytes. OncoImmunology *7*, e1412909. https://doi.org/10.1080/2162402X.2017.1412909.
70. Olson, K.E., Namminga, K.L., Lu, Y., Schwab, A.D., Thurston, M.J., Abdelmoaty, M.M., Kumar, V., Wojtkiewicz, M., Obaro, H., Santamaria, P., et al. (2021). Safety, tolerability, and immune-biomarker profiling for year-long sargramostim treatment of Parkinson's disease. EBioMedicine *67*, 103380. https://doi.org/10.1016/j.ebiom.2021.103380.
71. Gendelman, H.E., Zhang, Y., Santamaria, P., Olson, K.E., Schutt, C.R., Bhatti, D., Shetty, B.L.D., Lu, Y., Estes, K.A., Standaert, D.G., et al. (2017). Evaluation of the safety and immunomodulatory effects of sargramostim in a randomized, double-blind phase 1 clinical Parkinson's disease trial. NPJ Parkinsons Dis. *3*, 10. https://doi.org/10.1038/s41531-017-0013-5.
72. Baruch, K., Deczkowska, A., Rosenzweig, N., Tsitsou-Kampeli, A., Sharif, A.M., Matcovitch-Natan, O., Kertser, A., David, E., Amit, I., and Schwartz, M. (2016). PD-1 immune checkpoint blockade reduces pathology and improves memory in mouse models of Alzheimer's disease. Nat. Med. *22*, 135–137. https://doi.org/10.1038/nm.4022.
73. Lin, Y., Rajamohamedsait, H.B., Sandusky-Beltran, L.A., Gamallo-Lana, B., Mar, A., and Sigurdsson, E.M. (2019). Chronic PD-1 Checkpoint Blockade Does Not Affect Cognition or Promote Tau Clearance in a Tauopathy Mouse Model. Front. Aging Neurosci. *11*, 377. https://doi.org/10.3389/fnagi.2019.00377.
74. Latta-Mahieu, M., Elmer, B., Bretteville, A., Wang, Y., Lopez-Grancha, M., Goniot, P., Moindrot, N., Ferrari, P., Blanc, V., Schussler, N., et al. (2018). Systemic immune-checkpoint blockade with anti-PD1 antibodies does not alter cerebral amyloid-beta burden in several amyloid transgenic mouse models. Glia *66*, 492–504. https://doi.org/10.1002/glia.23260.
75. Kummer, M.P., Ising, C., Kummer, C., Sarlus, H., Griep, A., Vieira-Saecker, A., Schwartz, S., Halle, A., Brückner, M., Händler, K., et al. (2021). Microglial PD-1 stimulation by astrocytic PD-L1 suppresses neuroinflammation and Alzheimer's disease pathology. EMBO J. *40*, e108662. https://doi.org/10.15252/embj.2021108662.
76. Cheng, Y.Y., Chen, B.Y., Bian, G.L., Ding, Y.X., and Chen, L.W. (2022). Programmed Death-1 Deficiency Aggravates Motor Dysfunction in MPTP Model of Parkinson's Disease by Inducing Microglial Activation and Neuroinflammation in Mice. Mol. Neurobiol. *59*, 2642–2655. https://doi.org/10.1007/s12035-022-02758-x.
77. Sun, C., Mezzadra, R., and Schumacher, T.N. (2018). Regulation and Function of the PD-L1 Checkpoint. Immunity *48*, 434–452. https://doi.org/10.1016/j.immuni.2018.03.014.
78. Liu, Y., Yan, H., Gu, H., Zhang, E., He, J., Cao, W., Qu, J., Xu, R., Cao, L., He, D., et al. (2022). Myeloma-derived IL-32γ induced PD-L1 expression in macrophages facilitates immune escape via the PFKFB3-JAK1 axis. OncoImmunology *11*, 2057837. https://doi.org/10.1080/2162402X.2022.2057837.
79. Zhou, C., Wei, W., Ma, J., Yang, Y., Liang, L., Zhang, Y., Wang, Z., Chen, X., Huang, L., Wang, W., and Wu, S. (2021). Cancer-secreted exosomal miR-1468-5p promotes tumor immune escape via the immunosuppressive reprogramming of lymphatic vessels. Mol. Ther. *29*, 1512–1528. https://doi.org/10.1016/j.ymthe.2020.12.034.
80. Haderk, F., Schulz, R., Iskar, M., Cid, L.L., Worst, T., Willmund, K.V., Schulz, A., Warnken, U., Seiler, J., Benner, A., et al. (2017). Tumor-derived exosomes modulate PD-L1 expression in monocytes. Sci. Immunol. *2*, eaah5509. https://doi.org/10.1126/sciimmunol.aah5509.
81. Lin, X., Parisiadou, L., Sgobio, C., Liu, G., Yu, J., Sun, L., Shim, H., Gu, X.L., Luo, J., Long, C.X., et al. (2012). Conditional expression of Parkinson's disease-related mutant alpha-synuclein in the midbrain dopaminergic neurons causes progressive neurodegeneration and degradation of transcription factor nuclear receptor related 1. J. Neurosci. *32*, 9248–9264. https://doi.org/10.1523/JNEUROSCI.1731-12.2012.
82. Kamerkar, S., LeBleu, V.S., Sugimoto, H., Yang, S., Ruivo, C.F., Melo, S.A., Lee, J.J., and Kalluri, R. (2017). Exosomes facilitate therapeutic targeting of oncogenic KRAS in pancreatic cancer. Nature *546*, 498–503. https://doi.org/10.1038/nature22341.
83. Shelke, G.V., Lasser, C., Gho, Y.S., and Lotvall, J. (2014). Importance of exosome depletion protocols to eliminate functional and RNA-containing extracellular vesicles from fetal bovine serum. J. Extracell. Vesicles *3*, 24783. https://doi.org/10.3402/jev.v3.24783.
84. Qian, X., Nguyen, H.N., Song, M.M., Hadiono, C., Ogden, S.C., Hammack, C., Yao, B., Hamersky, G.R., Jacob, F., Zhong, C., et al. (2016). Brain-Region-Specific Organoids Using Mini-bioreactors for Modeling ZIKV Exposure. Cell *165*, 1238–1254. https://doi.org/10.1016/j.cell.2016.04.032.

STAR★METHODS

KEY RESOURCES TABLE

REAGENT or RESOURCE	SOURCE	IDENTIFIER
Antibodies		
anti-mouse CD63 mouse antibody	Santa Cruz Biotechnology	Cat# sc-5275; RRID: AB_627877
anti-mouse Alix antibody	Santa Cruz Biotechnology	Cat# sc-53540; RRID: AB_673819
anti-mouse TSG101 antibody	Santa Cruz Biotechnology	Cat# sc-7964; RRID: AB_671392
anti-mouse GAPDH antibody	Santa Cruz Biotechnology	Cat# sc-47724; RRID: AB_627678
anti-mouse L1CAM antibody	Abcam	Cat# ab24345; RRID: AB_448025
anti-mouse α-synuclein antibody	Thermo Fisher Scientific	Cat# AHB0261; RRID: AB_2536241
anti-mouse CD4 antibody	Abcam	Cat# ab288724; RRID: Not available
anti-mouse programmed death ligand 1	Thermo Fisher Scientific	Cat# 14-5983-82; RRID: AB_467784
anti-mouse Tyrosine Hydroxylase antibody	Santa Cruz Biotechnology	Cat# sc-25269; RRID: AB_628422
anti-human Tyrosine Hydroxylase polyclonal antibody	Thermo Fisher Scientific	Cat# OPA1-04050; RRID: AB_325653
anti-human Tyrosine Hydroxylase mouse antibody	Invitrogen	Cat# MA1-24654; RRID: AB_795666
anti-human PITX3 rabbit antibody	Invitrogen	Cat# 701181; RRID: AB_2532424
anti-human MAP2 chicken antibody	Novus Biologicals	Cat# NB300-213; RRID: AB_2138178
Monoclonal antibodies against mouse CD3	Biolegend	clone 145-2C11; RRID: AB_312667
Monoclonal antibodies against mouse CD4	Biolegend	clone GK1.5; RRID: AB_893324
Monoclonal antibodies against mouse T-bet	Biolegend	clone 4B10; RRID: AB_1595503
Monoclonal antibodies against mouse PD-L1	Biolegend	clone MIH7; RRID: AB_2728223
Monoclonal antibodies against mouse IFN-γ	Biolegend	clone XMG1.2; RRID: AB_961359
Monoclonal antibodies against mouse Ki67	Biolegend	clone 16A8; RRID: AB_11204254
Monoclonal antibodies against mouse PD-1	Biolegend	clone 29F.1A12; RRID: AB_1877231
Monoclonal antibodies against mouse CD45	Miltengy Biotec	clone 30F11; RRID: AB_2727922
Monoclonal antibodies against mouse CD3	Miltengy Biotec	clone REA641; RRID: AB_2801803
Monoclonal antibodies against mouse CD8	Miltengy Biotec	clone REA601; RRID: AB_2811550
Monoclonal antibodies against mouse CD62L	Miltengy Biotec	clone MEL14-H2.100; RRID: AB_2660514
Monoclonal antibodies against mouse CD25	Miltengy Biotec	clone 7D4; RRID: AB_2784088
Monoclonal antibodies against mouse IL-4	Miltengy Biotec	clone BVD4-1D11; RRID: AB_2660585
Monoclonal antibodies against mouse CD44	Miltengy Biotec	clone DB105; RRID: AB_2726111
Monoclonal antibodies against mouse GATA-3	Bioscience	clone TWAJ; RRID: AB_1963600
Goat anti-rabbit Alexa Fluor® 488 conjugated secondary antibody	Thermo Fisher Scientific	Cat# A-11008; RRID: AB_143165
anti-mouse cy3 secondary antibody	Jackson ImmunoResearch	Cat# 715-165-150; RRID: AB_2340813
anti-chicken cy5 secondary antibody	Jackson ImmunoResearch	Cat# 703-175-155; RRID: AB_2340365
Chemicals, peptides, and recombinant proteins		
recombinant mouse IL-2 protein	R&D Systems	Cat# 402-ML-020/CF
Dynabeads™ mouse T-activator CD3/CD28	Thermo Fisher Scientific	Cat# 11456D
recombinant mouse IL-12 protein	R&D Systems	Cat# 419-ML-010/CF
recombinant mouse IL-4 protein	R&D Systems	Cat# 404-ML-010/CF
recombinant mouse TGF-β protein	BioLegend	Cat# 763102
recombinant mouse IL-6 protein	R&D Systems	Cat# 406-ML-005/CF
2-Mercaptoethanol	Sigma-Aldrich	Cat# M6250-100mL
100 U/mL penicillin/streptomycin	Gibco™, Thermo Fisher Scientific	Cat# 15140122

(*Continued on next page*)

Continued

REAGENT or RESOURCE	SOURCE	IDENTIFIER
4′,6-diamidino-2-phenylindole (DAPI)	Thermo Fisher Scientific	Cat# D1306
protease inhibitor cocktail	Sigma-Aldrich	Cat# P2714
bovine serum albumin	Sigma-Aldrich	Cat# A1933-100G
BMS-1166	Selleck	Cat# S8859
lymphocyte separation medium	CEDARLANE	Cat# CL5030
Critical commercial assays		
MojoSort Mouse CD4 T cell Isolation Kit	BioLegend	Cat# 480006
MojoSort Mouse CD8 T cell Isolation Kit	BioLegend	Cat# 480008
PrimeScript™ RT reagent Kit with gDNA Eraser	TaKaRa	Cat# RR047A
Dil-Membrane EVs Labeling & Purification Kit	Rengen Biosciences	Cat# EXOPDil10-1
Experimental models: Cell lines		
Human iPSC lines carrying A53T mutant *SNCA*	NINDS Human Cell and Data Repository	Cat# ND50086; RRID: CVCL_RY37
Human iPSC lines carrying A53T mutation-corrected *SNCA*	NINDS Human Cell and Data Repository	Cat# ND50085; RRID: CVCL_RY36
SN4741 cell line	Emory University School of Medicine	RRID: CVCL_S466
HEK293T cell line	American Type Culture Collection	Cat# CRL-3216; RRID: CVCL_0063
H4 cell line	American Type Culture Collection	Cat# HTB-148; RRID: CVCL_1239
HMC3 cell line	American Type Culture Collection	Cat# CRL-3304; RRID: CVCL_II76
N9 cell line	A gift from Tangdu Hospital	RRID: CVCL_0452
Experimental models: Organisms/strains		
C57/BL6J WT mice	Jackson Laboratory, Bar Harbor, ME	RRID: IMSR_JAX:000668
PITX3 $^{+/IRES2-tTA}$ transgenic mice	Jackson Laboratory, Bar Harbor, ME	RRID: IMSR_JAX:021962
tetO-A53T transgenic mice	Jackson Laboratory, Bar Harbor, ME	RRID: IMSR_JAX:012442
Oligonucleotides		
NURR1 forward primer	This paper	Not available
NURR1 reverse primer	This paper	Not available
VMAT2 forward primer	This paper	Not available
VMAT2 reverse primer	This paper	Not available
GAPDH forward primer	This paper	Not available
GAPDH reverse primer	This paper	Not available
SRY forward primer	This paper	Not available
SRY reverse primer	This paper	Not available
Recombinant DNA		
pRK5 vector	This paper	Not available
pRK5-A53T-syn	This paper	Not available
Software and algorithms		
GraphPad Prism software (Version 8)	GraphPad Software Inc.	http://www.graphpad.com/scientific-software/prism/
Adobe Illustrator CS 6	Adobe Inc.	https://www.adobe.com/products/illustrator.html
ZetaView Software	Particle Metrix	https://particle-metrix.com/zetaview/

RESOURCE AVAILABILITY

Lead contact

Further information and requests for resources and reagents should be directed to and will be fulfilled by the lead contact, Zixu Mao (zmao@emory.edu).

Materials availability

The cell lines and plasmids used in this study are listed in the key resources table and are available from the lead contact on request.

Data and code availability

- The raw data for all blots are shown in Datas S1–S8.
- This paper does not report original code.
- Any additional information required to reanalyze the data reported in this paper is available from the lead contact upon request.

EXPERIMENTAL MODEL AND STUDY PARTICIPANT DETAILS

Mice

A53T-syn mice were bred by crossing PITX3 $^{+/IRES2-tTA}$ mice with tetO-A53T transgenic mice (Jackson Laboratory, Bar Harbor, ME). The protocols for the establishment of A53T-syn mice have been described previously.[81] C57/BL6J wild type mice were used as control. The mice were housed in a 12 h light/dark cycle and fed regular diet *ad libitum*. Both male and female mice were used in our animal experiments. Unless otherwise specified, 8-week-old A53T-syn mice or WT mice were investigated. All mouse experiments were approved by the Institutional Animal Care and Use Committees of Emory University.

METHOD DETAILS

Cell lines

HEK293T (Human Embryonic Kidney cell line, ATCC, CRL-3216), H4 (Human neuroglioma cell line, ATCC, HTB-148), and human embryonic microglia clone 3 (HMC3, ATCC, CRL-3304) cells were purchased from American Type Culture Collection (ATCC). The murine microglial cell line N9 was a kind gift from Dr. Qian Yang (Department of Experimental Surgery, Tangdu Hospital, the Fourth Military Medical University, Xi'an, Shaanxi, China). HEK293T, H4, and N9 cells were cultured in Dulbecco's Modified Eagle's Medium (DMEM) supplemented with 10% fetal bovine serum (FBS), 100 U/mL of penicillin, and 100 μg/mL of streptomycin. HMC3 cells were cultured in Modified Eagle's Medium (MEM) with 10% FBS, 100 U/mL of penicillin and 100 μg/mL of streptomycin. SN4741 cells were cultured in DMEM supplemented with 20% glucose and glutamine (200 mM). H4 and HMC3 cells were maintained at 37°C in a 5% CO_2 in incubator and SN4741 cells were maintained at 33°C in a 5% CO_2 incubator. For the purification of sEVs, the regular FBS in culture medium was replaced by sEV-depleted FBS. sEV-depleted FBS was prepared by ultracentrifuging the FBS for 16 h at 4°C and then filtered with a 100-nm filter as previously described.[82,83]

Reagents

The chemicals used in the study include recombinant mouse IL-2 protein (402-ML-020/CF, R&D Systems), Dynabeads mouse T-activator CD3/CD28 (11456D, Thermo Fisher Scientific), recombinant mouse IL-12 protein (419-ML-010/CF, R&D Systems), recombinant mouse IL-4 protein (404-ML-010/CF, R&D Systems), recombinant mouse TGF-β protein (763102, BioLegend), recombinant mouse IL-6 protein (406-ML-005/CF, R&D Systems), 2-Mercaptoethanol (M6250-100ML, Sigma-Aldrich), 100 U/mL penicillin/streptomycin (15140122, Gibco, Thermo Fisher Scientific), protease inhibitor cocktail (P2714, Sigma-Aldrich), bovine serum albumin (A1933-100G, Sigma-Aldrich), 4′,6-diamidino-2-phenylindole (D1306, Thermo Fisher Scientific), and BMS-1166 (S8859, Selleck).

Antibodies used in the study include anti-mouse CD63 mouse antibody (sc-5275, Santa Cruz Biotechnology), anti-mouse Alix antibody (sc-53540, Santa Cruz Biotechnology), anti-mouse TSG101 antibody (sc-7964, Santa Cruz Biotechnology), anti-mouse GAPDH antibody (sc-47724, Santa Cruz Biotechnology), anti-mouse L1CAM antibody (ab24345, Abcam), anti-mouse α-synuclein antibody (AHB0261, syn211, Thermo Fisher Scientific), anti-mouse programmed death ligand 1 (PD-L1) antibody (14-5983-82, MIH1, Thermo Fisher Scientific), anti-mouse tyrosine hydroxylase antibody (sc-25269, Santa Cruz Biotechnology), anti-human tyrosine hydroxylase polyclonal antibody (OPA1-04050, Thermo Fisher Scientific), anti-human tyrosine hydroxylase polyclonal antibody (AB152, Millipore), anti-human PITX3 polyclonal antibody (AB5722, Millipore), and anti-human MAP2 polyclonal antibody (NB300-213, Novus Biologicals). Monoclonal antibodies against mouse CD3 (clone 145-2C11), CD4 (clone GK1.5), T-bet (clone 4B10), PD-L1 (clone MIH7), IFN-γ (clone XMG1.2), Ki67 (clone 16A8), and PD-1 (clone 29F.1A12) were purchased from Biolegend; Monoclonal antibodies against mouse CD45 (clone 30F11), CD3 (clone REA641), CD8 (clone REA601), CD62L (clone MEL14-H2.100), CD25 (clone 7D4), IL-4 (clone BVD4-1D11), and CD44 (clone DB105) were purchased from Miltengy Biotec; Monoclonal antibody against mouse GATA-3 (clone TWAJ) was purchased from Bioscience.

Plasmids used in this study include pRK5 vector and pRK5-A53T-syn.

Transfection

The cells were cultured until they reached 70%–90% fluency for transfection. The culture medium was changed with sEV-depleted culture medium by replacing the regular FBS with sEV-depleted FBS. The culture media were collected for sEV purification 48 h after transfection.

DAergic neurons culture

Human iPSC lines carrying A53T mutant *SNCA* and A53T mutation-corrected *SNCA* were purchased from NINDS Human Cell and Data Repository. The protocols for the maintenance of iPSC lines and culture of midbrain DAergic neurons from human iPSC have been described in a

previous study.[84] In brief, cultured human iPSC colonies were detached with Collagenase Type IV and washed with fresh stem cell medium 7 days after passage. From day 1 to day 4, the iPSC lines were cultured on an Ultra-Low attachment 6-well plate containing EB medium composed of DMEM:F12, 15% Knockout Serum Replacer, 1 × Glutamax, 1 × 2-Mercaptoenthanol, 100 nM LDN-193189, 10 μM SB-431542, 100 ng/mL SHH (Peprotech), 2 μM Purmorphamine (Stemgent), 100 ng/mL FGF-8 (Peprotech). On day 5, the EB medium was switched to SHH medium, containing DMEM:F12, 1 × N2 Supplement, 1 × Glutamax, 100 nM LDN-193189, 3 μM CHIR99021, 100 ng/mL SHH, 2 μM Purmorphamine, 100 ng/mL FGF-8. From day 7 to day 13, SHH medium was replaced with induction medium, containing DMEM:F12, 1 × N2 Supplement, 1 × Glutamax, 100 nM LDN-193189, 3 μM CHIR99021. On day 14, 10–20 DAergic neurons were cultured in SpinΩ with differentiation medium, consisting of Neurobasal, 1 × B27 Supplement, 1 × Glutamax, 1 × 2-Mercaptoenthanol, 20 ng/mL BDNF, 20 ng/mL GDNF, 0.2 mM Ascorbic Acid, 1 ng/mL TGFβ, and 0.5 mM c-AMP. The culture media of midbrain DAergic neurons were collected on day 28 when the DAergic neurons matured.

sEV extraction from cell culture medium

The sEVs from cell culture were extracted using sequential centrifugation process as previously reported.[38] Briefly, the culture media were collected and subsequently subjected to sequential centrifugation steps at 300 g for 5 min, 800 g for 5 min, and 2,000 g for 10 min to remove cells and cell debris. The supernatant was further centrifuged by 10,000 g for 30 min at 4°C to remove large EVs. The sEVs were purified by ultracentrifugation at 110,000 g and 4°C for 70 min, washed with 1 × PBS, and re-centrifugated under the same condition.

NEEVs extraction from mouse plasma

NEEVs were isolated from mouse plasma using antibody-coated superparamagnetic microbeads following the protocol as previously described.[33,57] Briefly, a protease inhibitor cocktail (Sigma-Aldrich) was added to mouse plasma sample (>300 μL) followed by centrifugation at 4°C and 2000× g for 15 min. The supernatant was transferred to a new tube and centrifuged at 4°C and 12000× g for 30 min. Then 10 mg M-270 Epoxy beads from a Dynabeads Antibody Coupling Kit (Life Technologies, Grand Island, NY, USA) were coated with 100 μg anti-mouse L1CAM (Abcam) or normal mouse IgG (Santa Cruz Biotechnology Inc.) according to the manufacturer's instructions. The supernatant (300 μL) was diluted at a ratio of 1:3 with 600 μL phosphate buffered saline (PBS) (pH 7.4) and incubated with 1 mg of antibody-coated beads at 4°C for ~24 h with gentle rotation. Before elution, the beads were washed four times with 0.1% bovine serum albumin (BSA)/PBS (pH 7.4). NEEVs were eluted from the beads with 140 μL 0.1 M glycine (pH 3) plus 10 μL of 1 M Tris buffer (pH 7) for 1 h at room temperature with gentle shaking. Isolated NEEVs were fixed using a fixing buffer (4% paraformaldehyde (PFA)/5% glutaraldehyde) for transmission electron microscopy (TEM) imaging. For detection of sEV markers by western blot, the sEV proteins were extracted by incubating the beads with 110 μL 0.1% BSA/PBS (pH7.4) containing Triton X-100 (1%) and protease and phosphatase inhibitors for 1 h at room temperature with gentle shaking.

Nanoparticle tracking analysis

The culture media were collected 48 h after transfection to perform nanoparticle tracking analysis (NTA) of sEVs released by cultured cell lines using ZetaView Nanoparticle Tracking Analyzer. Media were subjected to sequential centrifugation steps at 800 g for 5 min and 2,000 g for 10 min to remove cells and cell debris. The supernatant was centrifuged by 10,000 g for 30 min at 4°C to deplete large EVs. Before NTA, the supernatant was diluted in PBS to a final volume of 1 mL. Each measurement was conducted by scanning 11 cell positions and capturing 60 frames per position with following parameters: Focus: autofocus; Camera sensitivity for all samples: 65.0; Shutter: 70; Scattering Intensity: 4.0; Cell temperature: 25°C. The captured videos were analyzed by ZetaView Software (Particle Metrix) with specific analysis settings: Maximum particle size: 1000, Minimum particle size 5, Minimum particle brightness: 20. Hardware: embedded laser: 40 mW at 488 nm. The median particle diameter and mean concentrations were obtained after NTA of sEV samples.

Western blot

Whole cell lysates were prepared in SDS containing sample buffer (31.5 mM Tris-HCl, pH 6.8, 10% glycerol, 1% SDS, and 0.005% bromophenol blue) and equal protein amounts of lysates (20–30 μg) were separated by 10–15% SDS-PAGE gel at 100 V for 1.5 h. Proteins were transferred to polyvinylidene difluoride membrane at 25 V for 1.5 h using a half-dry blotting system (Bio-Rad Laboratories). Blots were probed by incubation with primary antibodies (1:1,000) overnight at 4°C, washed three times, and then incubated with the secondary antibodies (1:10,000) at room temperature for 1 h. Images were developed in an M35A X-OMAT Processor system (Kodak) using ECL reagent (GE Healthcare).

Transmission electron microscopy

Purified sEVs were fixed with 1 mL of 4% PFA for 5 min. Five - seven μL sEV suspension solution was loaded on the grid and incubated for 1 min. Twenty drops of filtered 1% uranyl acetate (UA) were applied to the EM grid. After removing the excess UA solution, the grid was rinsed with a drop of water, and placed on the table for 10 min at room temperature. The grid was imaged by TEM at 80 kV.

Isolation of mouse spleen cells, $CD4^+$ T cells, and $CD8^+$ T cells

Single-cell spleen lymphocyte suspensions were obtained from spleens of 8-week-old A53T-syn transgenic mice or WT mice using the lymphocyte separation medium according to the manufacturer's instructions (CL5030, CEDARLANE). For the purification of $CD4^+$ and $CD8^+$ T cells, non-$CD4^+$ cells and non-$CD8^+$ cells were removed by negative selection using MojoSort Mouse CD4 T or CD8 T cell Isolation

Kits according to the protocols provided by manufacture (BioLegend). The purity of $CD4^+$ T cells and $CD8^+$ T cells was determined using flow cytometry. For isolation of naive $CD4^+$ T cells ($CD4^+CD25^-CD44^{low}CD62L^{high}$), purified $CD4^+$ T cells were further sorted using antibodies to mouse CD4-APC, CD25-FITC, CD44-PE, and CD62L-PE-Cy7 by flow cytometry. Purity of $CD4^+CD25^-CD44^{low}CD62L^{high}$ T cells after isolation was over 97%.

Culture of mouse spleen cells, $CD4^+$ T cells, and $CD8^+$ T cells

Isolated mouse spleen cells, $CD4^+$, and $CD8^+$ T cells were cultured in 24-well flat bottom plates (0.5×10^6 cells per well) in 0.5 mL of complete RPMI 1640 media supplemented with 10% sEV-depleted FBS, 200 mM L-glutamine, 100 U/mL penicillin/streptomycin and 55 mM 2-Mercaptoethanol (RP-10). Mouse T-Activator αCD3/αCD28 beads and 50 ng/mL recombinant mouse IL-2 were added to the culture medium for long term maintenance. The cells were cultured for 24 h before sEV treatment.

Differentiation induction of mouse naive $CD4^+$ T cells

Isolated mouse naive $CD4^+$ T cells were cultured in 24-well plates (0.5×10^6 cells per well) in 0.5 mL of complete RPMI 1640 media supplemented with 10% sEV-depleted FBS, 200 mM L-glutamine, 100 U/mL penicillin/streptomycin and 55 mM 2-Mercaptoethanol in the presence of Mouse T-Activator αCD3/αCD28 beads in addition to 50 ng/mL recombinant mouse IL-2. Cells were cultured under Th1 (50 ng/mL recombinant IL-12 and 10 mg/mL anti-IL-4), Th2 (50 ng/mL recombinant IL-4 and 10 mg/mL anti-IFN-γ), Th17 (10 ng/mL recombinant TGF-β, 100 ng/mL recombinant IL-6, 10 mg/mL anti-IFN-γ and 10 mg/mL anti-IL-4) or iTreg (10 ng/mL recombinant TGF-β) conditions. The naive cells were cultured for 24 h under different conditions before sEV treatment.

sEVs labeling and internalization

sEVs (30–50 μg) isolated from SN4741 cells were labeled with Dil lipophilic dye according to the instruction manual of Dil-Membrane EVs Labeling & Purification Kit (Rengen Biosciences, EXOPDil10-1). After incubation at 37°C for 30 min, the excess unbound dye was removed through the Spin Columns. Purified mouse $CD4^+$ T cells (5×10^4) were incubated with Dil-labeled EVs (10 μg) for 24 h, and then fixed in 4% paraformaldehyde (PFA) for 10 min at room temperature, washed 1× with PBS, and then incubated with rabbit anti-mouse CD4 primary antibody (1:50; Abcam) overnight. The cells were washed 3× with PBS and incubated with goat anti-rabbit Alexa Fluor 488 conjugated secondary antibodies (1:1000; Thermo Fisher Scientific) at room temperature for 2 h. After washing 3× with PBS, the cells were incubated with DAPI (1:1000; Thermo Fisher Scientific) for 5 min at room temperature and subjected to confocal microscopy using a Zeiss LSM 780 confocal microscope.

sEVs treatment

For most of sEVs treatment experiments, 5 μg sEVs were added into the culture medium of mouse splenocytes or purified $CD4^+$ or $CD8^+$ T cells for 48 h (The final concentration of sEVs in medium is 10 μg/mL). To observe the dose-effect relationship, varying amounts of sEVs (20–30 μg/mL) were used. For differentiation assay, cells were treated with sEVs for 96 h.

Blocking of PD-L1

To block PD-L1 and PD-1 interaction, anti-PD-L1 antibody (4 μg/mL for final concentration; clone MIH-1; Thermo Fisher Scientific)[44] or BMS-1166 (1 μM for final concentration; S8859, Selleck),[43] was added into the $CD4^+$ and $CD8^+$ T cell culture media before the treatment of sEVs.

Flow cytometry

Cytokines, transcription factors, and surface markers of T cells were evaluated by flow cytometry with a FACSCanto II Cell Analyzer (BD Biosciences) following the recommended protocols by eBioscience. To detect intracellular expression of INF-γ, IL-4, and IL-17A in $CD4^+$ or $CD8^+$ T cells, cells were first treated with 1 μg/mL ionomycin (Sigma), 50 ng/mL phorbol 12-myristate 13-acetate (PMA, Sigma), and 2 μg/mL Brefeldin A (BioLegend) for 4–6 h at 37°C before flow cytometry analysis.

Immunocytochemistry

DAergic neurons differentiated from iPSC were cultured on the glass coverslip (Corning Incorporated) with 24-well plates and stained for immunocytofluorescence as described.[84] The primary antibodies used in immunofluorescence included: anti-human TH mouse antibody (1:400; MA1-24654, Invitrogen), anti-human PITX3 rabbit antibody (1:500; 701181, Invitrogen), and anti-human MAP2 chicken antibody (1:400; NB300-213, Novus). The secondary antibodies used were shown in key resources table. Images were acquired with an Olympus DP70 fluorescent microscopy (Olympus Corporation, Japan).

RNA isolation, RT-PCR, and RT-qPCR

For the sex identification of SN4741 cell line, total RNA of SN4741 cells and N9 cells (male origin) was selectively isolated away from proteins and DNA using the Trizol reagent. Contaminating DNA was then removed from the RNA using gDNA Eraser contained in PrimeScriptTM RT reagent Kit (RR047A; TaKaRa) according to the instruction manual. The purified total RNA was reverse-transcribed into complementary DNA

(cDNA) using the same PrimeScriptTM RT reagent Kit (RR047A; TaKaRa). After reverse transcription, the cDNA was quantified and its purity was validated using a NanoDrop Spectrophotometer (Thermo Scientific, New York). *GAPDH* was used as a housekeeping gene to confirm the successful amplification of cDNA using forward primer 5′-GTT GAA GTC GCA GGA GAC AA-3′ and 5′-GGG TGT GAA CCA CGA GAA ATA-3′ in the reverse. The male-specific genetic marker *SRY* gene[58,59] was amplified by standard PCR using forward primer 5′-TTG TCT AGA GAG CAT GGA GGG CCA T-3′ and 5′-CCA CTC CTCT GT GAC ACT TTA GCC CT-3′ in the reverse. The PCR reaction started at 95°C for 30 s, included 35 cycling reactions of 95°C for 15 s/62°C for 15 s/72°C for 30 s, and was followed by a single reaction at 72°C for 5 min. The standard PCR was performed using the Bio-Rad PCR System. The PCR products were then separated on a 1% agarose-TAE ethidium bromide gel, for 30 min at a constant voltage of 100V. Bands were visualized with a ChemiDoc MP Imaging System (Bio-Rad). The *GAPDH* locus ran at about 500 bp as expected and the *SRY* locus ran at 100 bp.

For the measurement of DAergic neuron-specific markers (*NURR1* and *VMAT2*) using RT-qPCR, total RNA of human DAergic neurons was isolated with Trizol reagent according to the manufacturer's instructions (Invitrogen). A total of 1 μg RNA was utilized to synthesize cDNA with a SuperScript III First-Strand Synthesis System (Invitrogen). cDNA was quantified with qPCR via TaqMan assay (Invitrogen). The human *NURR1* gene was amplified using forward primer 5′-AAC TGC ACT TCG GCA GAG TT-3′ and 5′- AAA GCA ATG GGG AGT CCA GC-3′ in the reverse. The human *VMAT2* gene was amplified using forward primer 5′-TCC TGT TCA TCG TGT TCC TGG-3′ and 5′-CTG GCC GTC TGG ATT TCT GTA-3′ in the reverse. Expression levels of *NURR1* and *VMAT2* were analyzed following the ΔΔCt method using *GAPDH* as a normalization control.

QUANTIFICATIONS AND STATISTICAL ANALYSIS

Statistical analyses

Statistical analysis was performed with GraphPad Prism software (Version 8). A two-tailed unpaired Student's t test was used for statistical analysis of two groups. One-way analysis of variance (ANOVA) with Tukey's multiple comparisons test was used to compare the means of three or more groups. Two-way ANOVA followed by Tukey's multiple comparisons test was used to evaluate data with two factors. A p-value <0.05 was considered statistically significant. All collected data was analyzed and provided as mean $\pm$ SEM. Unless otherwise specified, all experiments were replicated three times with representative images or data shown in the figures.